



HAL
open science

Stabilization of β -catenin promotes melanocyte specification at the expense of the Schwann cell lineage

Sophie Colombo, Valérie Petit, Roselyne Wagner, Delphine Champeval, Ichiro Yajima, Franck Gesbert, Zackie Aktary, Irwin Davidson, Véronique Delmas,
Lionel Larue

► To cite this version:

Sophie Colombo, Valérie Petit, Roselyne Wagner, Delphine Champeval, Ichiro Yajima, et al.. Stabilization of β -catenin promotes melanocyte specification at the expense of the Schwann cell lineage. Development (Cambridge, England), 2022, 149 (2), pp.dev194407. 10.1242/dev.194407 . hal-03780846v1

HAL Id: hal-03780846

<https://hal.science/hal-03780846v1>

Submitted on 5 Oct 2022 (v1), last revised 2 Oct 2023 (v2)

HAL is a multi-disciplinary open access archive for the deposit and dissemination of scientific research documents, whether they are published or not. The documents may come from teaching and research institutions in France or abroad, or from public or private research centers.

L'archive ouverte pluridisciplinaire **HAL**, est destinée au dépôt et à la diffusion de documents scientifiques de niveau recherche, publiés ou non, émanant des établissements d'enseignement et de recherche français ou étrangers, des laboratoires publics ou privés.

Stabilization of β -catenin promotes melanocyte specification at the expense of the Schwann cell lineage

Sophie COLOMBO¹⁻³#, Valérie PETIT¹⁻³§, Roselyne Y WAGNER¹⁻³,
Delphine CHAMPEVAL¹⁻³, Ichiro YAJIMA¹⁻³, Franck GESBERT¹⁻³, Zackie AKTARY¹⁻³,
Irwin DAVIDSON^{3,4}, Véronique DELMAS¹⁻³, and Lionel LARUE^{1-3*}

(1) Institut Curie, PSL Research University, INSERM U1021, Normal and Pathological Development of Melanocytes, Orsay, France,

(2) Univ Paris-Sud, Univ Paris-Saclay, CNRS UMR 3347, Orsay, France,

(3) Equipes Labellisées Ligue Contre le Cancer

(4) Institut de Génétique et de Biologie Moléculaire et Cellulaire, CNRS/INSERM/UNISTRA, 1 Rue Laurent Fries, 67404 Illkirch Cedex, France. Department of Functional Genomics and Cancer.

Current address: Dynacure, Bioparc 3, 850 Boulevard Sébastien Brant, 67400 Illkirch, France

§ These authors contributed equally to the work

* Corresponding author: E-MAIL: lionel.larue@curie.fr

Key words: pigmentation, cell fate, determination, proliferation, *Mitf*, *FoxD3*

Summary statement

Activation of β -catenin in bipotent Schwann-cell precursors during a specific developmental window induces *MITF* and represses *FoxD3* to promote melanoblast cell fate at the expense of Schwann cells in limbs.

Abstract

The canonical *Wnt*/ β -catenin pathway governs a multitude of developmental processes in various cell lineages, including the melanocyte lineage. Indeed, β -catenin regulates *Mitf-M* transcription, the master regulator of this lineage. The first wave of melanocytes to colonize the skin is directly derived from neural crest cells, while the second wave of melanocytes is

derived from Schwann-cell precursors (SCPs). We investigated the influence of β -catenin in the development of melanocytes of the first and second waves by generating mice expressing a constitutively active form of β -catenin in cells expressing tyrosinase. Constitutive activation of β -catenin did not affect the development of truncal melanoblasts but led to marked hyperpigmentation of the paws. By activating β -catenin at various stages of development (E8.5-E11.5), we showed that the activation of β -catenin in bipotent SCPs favored melanoblast specification at the expense of Schwann cells in the limbs within a specific temporal window. Furthermore, *in vitro* hyperactivation of the Wnt/ β -catenin pathway, which is required for melanocyte development, induces activation of Mitf-M, in turn repressing FoxD3 expression. In conclusion, β -catenin overexpression promotes SCP cell fate decisions towards the melanocyte lineage.

INTRODUCTION

Multipotent neural-crest cells (NCC) in vertebrates constitute a transient population of cells arising from the dorsal part of the neural tube (Le Douarin and Kalcheim, 1999) that gives rise to numerous derivatives, such as neuronal and glial cells of the peripheral nervous system (PNS), smooth muscle cells, and melanocytes. Melanocytes produce melanin, a tyrosine-based polymer, in specialized organelles, the melanosomes. Classical melanocytes are pigmented cells, which (i) are found in the skin (dermis or epidermis), (ii) are involved in skin pigmentation, and (iii) are differentiated from melanoblasts derived from late-migrating NCC that have followed the dorso-lateral migratory pathway between the dermamyotome and the overlying ectoderm. These melanoblasts, referred to as first-wave melanoblasts, are specified as early as E8.5, before they start migrating along the dorso-lateral pathway from E10.5 (Petit and Larue, 2016). Between E11.5 and E13.5, most melanoblasts enter the epidermis, where they actively proliferate (Luciani et al., 2011). Between E15.5 and E17.5, epidermal melanoblasts migrate towards the forming hair follicles. In the furry parts of adult mice, most melanocytes are found in the hair matrix, whereas only few interfollicular melanocytes remain in the epidermis after birth (Hirobe, 1984). Epidermal melanocytes are abundant in the hairless parts of the body, such as the tail and paws (Silvers, 1979), except in the palms and soles, which have very few (Kunisada et al., 1998) and (Fig. S1). Melanocytes are considered to be non-classical if they are found in organs other than skin, not involved in skin pigmentation, and/or have not followed the dorso-lateral migratory pathway during development (Colombo et al., 2011). However, two types of non-classical melanocytes involved in skin pigmentation have been found, although they did not follow the dorso-lateral migratory route. One corresponds to a population of cells originating around the time of gastrulation, most likely within the mesoderm, and ultimately residing within the

dermis (Kinsler and Larue, 2018). These melanoblasts are referred to as “mesodermal-wave melanoblasts”. The other is derived from Schwann cell precursors (SCPs) and is referred to as second-wave melanoblasts. SCPs are multipotent embryonic progenitors covering all developing peripheral nerves and originate from early ventrally-migrating NCC (Furlan and Adameyko, 2018). Previous studies have shown that a significant number of melanocytes in the skin of the trunk and limbs are produced from SCPs adjacent to spinal nerves that innervate the skin during development. Additionally, it was shown that the glial *versus* melanocyte fate is highly dependent on nerve contact (Adameyko et al., 2009). The authors showed that SCP-derived melanoblasts migrating ventrally from the DRG are specified around E11 in the mouse. While multiple elegant experiments had shown that the melanocytes and Schwann-cells share a common glial-melanogenic bipotent precursor and can be transdifferentiated into each other *in vitro* (Dupin et al., 2000; Dupin et al., 2003; Nitzan et al., 2013b; Real et al., 2006), the factors controlling the cell fate decisions between these two lineages remained unclear. More recent experiments started elucidating the molecular pathways involved in the glial-melanocyte switch. Those bipotent progenitors express various proteins including Sox2, Sox9, Sox10, Fabp, Mitf, Pax3 and FoxD3 (Adameyko and Lallemand, 2010). It has been shown that FoxD3 represses the expression of *Mitf* in zebrafish (Curran et al., 2009), in melanoma cell lines and cultured quail neural crest (Abel et al., 2013; Thomas and Erickson, 2009). Moreover, the downregulation of *FoxD3* is necessary for SCPs to follow a melanocyte fate (Adameyko et al., 2012; Jacob, 2015; Nitzan et al., 2013b).

β -catenin plays critical roles in multiple developmental processes, such as proliferation and cell fate decisions, owing to its dual function in cadherin-dependent cell-cell interactions and as a central component of the canonical Wnt signaling pathway (Aktary et al., 2016; Steinhart and Angers, 2018). Gain-of-function studies have shown induction of cellular proliferation of a number of cell types in transgenic mice expressing stabilized β -catenin (Gat et al., 1998; Imbert et al., 2001; Romagnolo et al., 1999). This pathway influences early melanoblast development, mainly through various common β -catenin/LEF targets, including Myc and Ccdn1, and a major downstream target of β -catenin in the melanocyte lineage, the Mitf-M transcription factor (Luciani et al., 2011). Mitf-M exerts survival and proliferation functions during the expansion of melanoblasts from the neural crest (Carreira et al., 2006; Hornyak et al., 2001) and regulates melanocyte differentiation by inducing the key enzymes of melanogenesis Tyr, Tyrp1, and Dct (Steingrimsson et al., 2004). The deletion of β -catenin specifically in migrating melanoblasts leads to hypoproliferation due to reduced Mitf-M expression (Luciani et al., 2011). Both the temporal and spatial fine-tuning of β -catenin and Mitf-M levels is required to regulate their various

downstream targets and generate the required number of melanoblasts at the correct location during development. Apart from its role in neural crest induction and expansion, the Wnt/ β -catenin signaling pathway has been implicated in neural-crest cell fate decisions. Mice deficient for both *Wnt1* and *Wnt3a* exhibit a marked deficiency of Dct-positive neural-crest-derived melanoblasts (Ikeya et al., 1997). β -catenin has also been directly associated with melanoblast cell-fate specification in various species using β -catenin gain- and loss-of-function approaches. In zebrafish, injection of *β -catenin* mRNA into a subpopulation of migrating NCCs induces the formation of pigmented cells (Dorsky et al., 1998). In mice, the conditional ablation of *β -catenin* in premigratory NCCs leads to a loss of melanocytes and sensory neurons (Hari et al., 2012), whereas its activation promotes the formation of the sensory neuronal lineage at the expense of other neural-crest derivatives (Lee et al., 2004). A change in cell-fate specification, rather than a proliferation defect, underlies the loss of melanocytes. Moreover, the expression of a constitutive activated form of β -catenin in bipotent cardiac neural-crest cells, known to produce mainly smooth muscle cells and few melanocytes, promotes the melanocyte fate at the expense of the smooth-muscle fate in the *ductus arteriosus* of embryonic hearts, leading to patent ductus arteriosus, a congenital disease (Yajima et al., 2013). Overall, these results demonstrate the essential role of the Wnt/ β -catenin pathway in NCC and melanocyte fate determination.

We investigated the influence of β -catenin on the first- and second-wave of melanocyte development. A mouse genetic approach was used to express a conditional mutant of β -catenin (β cat Δ ex3), known to be hyperactive (Harada et al., 1999), at specific times and in specific neural-crest-cell derivatives using either constitutive or inducible Cre lines under the control of the Tyrosinase promoter (Delmas et al., 2003; Yajima et al., 2006). It has already been shown that the use of the Tyr::Cre transgene, to conditionally delete specific genes, is targeting the melanocytic lineage but also the enteric nervous system, smooth muscle cells in the heart, and the Schwann cell lineage (Puig et al., 2009; Radu et al., 2019; Yajima et al., 2013). We observed that constitutive activation of β -catenin led to hyperpigmentation of the paws due to promotion of the melanocyte fate at the expense of the glial fate at the time of SCP specification. At the molecular level, we show that β -catenin overexpression represses *FoxD3* expression through *Mitf*, thereby allowing SCPs to follow a melanocyte fate.

RESULTS

Constitutively active β -catenin (β cat Δ ex3) induces hyperpigmentation of the paws

On a C57BL/6 background, we generated mice producing a constitutively active form of β -catenin (Tyr::Cre^o; β catex3^{flox/+} = β cat Δ ex3) in cells of the Tyr::Cre lineage by crossing Tyr::CreA mice (Delmas et al., 2003) with mice harboring a floxed exon 3 of β -catenin (Harada et al., 1999; Yajima et al., 2013). β cat Δ ex3 mutant mice displayed strong hyperpigmentation of the palms and soles with full penetrance (Figs. 1A, S2A). However, we did not observe strong hyperpigmentation on the back of the paws (Fig. S2A). Palmoplantar hyperpigmentation was already present at birth and was particularly striking at P5 (Fig. 1A). Transversal sections at the metatarsal level of paws from post-natal day 1 (P1) and P5 newborn mice revealed high levels of pigmentation on the ventral side of the β cat Δ ex3 mutant paws, whereas it was absent from the wild-type (WT) paws (Figs. 1B, S2B). Moreover, this pigmentation was localized in the dermis, directly under the epidermis, as well as more deeply in the palmoplantar mesenchyme.

β -catenin is properly defloxed and activated in β cat Δ ex3 melanoblasts and melanocytes

The transcriptional activity of β cat Δ ex3 was previously assessed with the “TOP and FOP” flash luciferase reporter assay and was shown to be five times higher than that of WT β -catenin (Yajima et al., 2013). Deletion of exon3 in β cat Δ ex3 mice was verified by PCR on genomic DNA extracted from mouse tails containing melanocytes (Fig. S3A,B). We verified the presence of β -catenin in the nucleus, a marker of its stabilization/activation, by immunofluorescence of skin sections during development and after the birth of Tyr::Cre^o; Dct::LacZ (WT-LacZ) and Tyr::Cre^o; β catex3^{flox/+}; Dct::LacZ (β cat Δ ex3-LacZ) mice using β -galactosidase expression as a melanoblast/melanocyte marker (MacKenzie et al., 1997; Yajima et al., 2013). β -catenin was present in the nucleus of β cat Δ ex3 melanoblasts in the epidermis of E14.5 embryos whereas it was localized at the membrane in WT mice (Fig. S3C). These results show that β -catenin was properly defloxed and activated in β cat Δ ex3 melanoblasts and melanocytes.

The β cat Δ ex3 mutation does not affect coat color nor truncal melanoblast proliferation

β cat Δ ex3 mutant mice have no distinctive coat color, ear, or tail phenotype (Fig. S4A). The mutation of β -catenin is induced around E9.0, as the Tyr::Cre transgene begins to be expressed, after dorso-laterally-migrating melanoblasts have been determined. We evaluated the number of WT-LacZ and β cat Δ ex3-LacZ melanoblasts in the truncal region of

E13.5 to E18.5 embryos. From E13.5 to E15.5, the number of melanoblasts was determined on whole mount embryos stained with X-gal in a region localized between the fore- and hind-limbs (ranging from approximately somite 13 to somite 25). There was no significant difference in melanoblast numbers at these stages between WT and mutant embryos (Fig. S4B). At E16.5 and E18.5, truncal melanoblasts were counted on embryo sections immunostained for β -galactosidase (Fig. S4C). Few or no melanoblasts were present in the dermis at these stages, as previously described for WT embryos (Luciani et al., 2011). The presented figures correspond to epidermal and hair-follicle melanoblasts. At E16.5, hair follicles have just initiated invagination from the epidermis while at E18.5, they extend into the dermis and numerous melanoblasts can be found entering and within the hair follicles. There was no difference in melanoblast numbers between WT and mutant mice at these two stages (Fig. S4C). We also investigated melanoblast proliferation in the skin of the trunk using bromodeoxyuridine (BrdU) incorporation assays on embryos collected at E16.5 and E18.5. There was no significant difference in the percentage of BrdU-positive melanoblasts at these stages (Fig. S4D). Overall, these results show that hyperactivation of β -catenin does not influence the development of already determined dorso-laterally-migrating melanoblasts.

Hyperpigmentation of β cat Δ ex3 ventral paws is due to an elevated number of melanocytes

X-gal staining of transversal sections of P1 WT-LacZ and β cat Δ ex3-LacZ paws revealed numerous Dct-positive cells colocalized with strong pigmentation in the mutant palms and soles, whereas they were absent in WT littermates (Fig. 2A,B). X-gal staining also labeled the nerves in the posterior paws (Fig. 2B), but not in the anterior paws (Fig. 2A) (MacKenzie et al., 1997). These nerve-associated Dct::LacZ positive-cells were most likely melanoblasts and/or bipotent SCP and not nerve projections, as we observed a similar pattern of Dct-positive cells colocalized with pigment in both the anterior and posterior paws. The pigmentation pattern in mutant paws was located around the nerves, most likely following nerve projections (Fig. 2B). In the phalanges, pigmentation was strikingly localized around the bones of the digits (Fig. 2B), whereas at the metacarpal/metatarsal level, it was mostly localized under the epidermis (Fig. 2A). We followed the expression of GFP (corresponding to the cells that were defloxed by Cre) and Tuj1 (used as a marker for neuronal cells) in Tyr::Cre^o ; ZEG^o E14.5 embryo. We observed that some cells are close from one to another being GFP or Tuj1 positive in the ventral part of the limbs. This double labelling revealed that defloxed cells are closed to neurons (Fig.3A-C). Moreover, we performed the staining of Pmel and Tuj1 in paws transversal sections revealing that some Pmel-positive cells are in

close proximities with Tuj1-positive cells (Fig.3D-K). These results suggest that ectopic melanocytes are present in the mutant paws.

Hyperpigmentation of β cat Δ ex3 ventral paws is due to abnormal invasion of melanoblasts during development

The β cat Δ ex3 paw phenotype was already visible at birth, when the mice are normally unpigmented. It is thus likely the consequence of altered developmental processes. We analyzed the location and number of melanoblasts in E13.5 limbs and paws, when melanoblasts have started their migration to the limbs but have not yet reached the paws. There was no difference in melanoblast distribution between WT and mutant embryos at this stage (Fig. S5A). A difference started to appear at E14.5. Anterior mutant paws displayed melanoblasts ventrally in the palms, as well as few melanoblasts dorsally, whereas they were not present or in very low numbers in WT embryos (Figs. 4A, S5B). There was a statistically significant increase in the number of Dct-positive melanoblasts in the distal region of the ventral limbs, but not in the proximal region of the limb (Fig. 4C). While there was a tendency to increased numbers also on the dorsal side of mutant paws, the difference was not statistically significant (Fig. 4C). No phenotype was yet visible in the posterior paws at this stage (not shown). At E15.5, the phenotype was clearly visible ventrally in mutant paws. Large numbers of melanoblasts were found in the palms and soles and proximal part of the digits, whereas they were mostly absent from the WT paws. Melanoblasts could also be seen in the digits on the dorsal side of the paws (Figs. 4B, S5C). In WT mice, a clear front of migration of melanoblasts was apparent at the junction between the limb and paw (Figs. 4A, S5, black dotted lines). In mutant mice, however, melanoblasts appeared to cross this junction and continue their migration into the palms, soles, and digits. Altogether, these results suggest that constitutively active β -catenin during the establishment of the melanocyte lineage induces melanoblast colonization into the palms and soles.

Melanocytes from the palms and soles originate from the second wave of melanoblasts.

Melanocytes are specified from the neural crest around E8.5-E9.0 (Le Douarin and Kalcheim, 1999), while they seem to specify from SCPs around E10.5-E11.5 (Fig. S6) (Adameyko et al., 2009; Van Raamsdonk and Deo, 2013). We used temporal induction of β cat Δ ex3 to reveal the origin of the melanoblasts invading the soles and palms and leading to the hyperpigmentation phenotype. We generated Tyr::CreER^{T2/0}; β catex3^{flox/+} mice (β cat Δ ex3-Tam), induced activated β -catenin at either E8.5, E10.5 or E11.5 with tamoxifen, and evaluated the location and number of melanoblasts in the distal part of the limbs at

E15.5. The tamoxifen induction at E8.5 and E11.5 appeared to affect neither the number nor localization of melanoblasts at E15.5 in the distal region of the ventral paws (Figs. 4D,F,G,I). However, tamoxifen induction at E10.5 resulted in a clear increase in the number of melanoblasts in the distal region of the ventral paws (Figs. 4E,H). These results suggested that bipotent SCPs may specify into melanocytes as early as E10.5 when the level of β -catenin is higher than normal. We followed the expression of Gfp (corresponding to the cells that were defloxed) and Gfap (used as a marker for Schwann cells and Schwann cell precursors) in E14.5 embryo after Cre recombination of the ZEG transgene. We observed that cells are both Gfp and Gfap positive in the ventral part of the limbs. This double labelling revealed that Gfap positive cells expressed or are derived from a cell that produced Cre under the control of the tyrosinase promoter (Fig. 5). We thus estimated the number of Schwann cells (Gfap-positive cells) and melanoblasts (Mitf-positive cells) in β cat Δ ex3 limbs. Expression of β cat Δ ex3 led to an increased number of melanoblasts and a decreased number of Schwann cells in the palms (Fig. 6). These results suggested that the expression of a constitutively active form of β -catenin in glial-melanogenic bipotent progenitors at the time of their fate determination promoted their differentiation into melanoblasts of the second wave at the expense of glial cells. Because SCPs are located along and migrate with axons of peripheral nerves, the ectopic melanocytes observed in the paws of β cat Δ ex3 mice would likely have migrated away from these nerves.

β -catenin induces the transcription of Mitf and the repression of FoxD3

The downregulation of *FoxD3* in SCPs is necessary to allow emergence of melanocyte cells (Adameyko et al., 2012; Jacob, 2015; Nitzan et al., 2013a) prompting us to ask whether activation of β -catenin signaling affected *FoxD3* expression. Constitutive activation of β -catenin signaling by knocking down *APC* using an siRNA in HEI-193 human schwannoma (Fraenzer et al., 2003) and IPN 02.3 Schwann (Li et al., 2016) cell lines resulted in a significant decrease of *FOXD3* mRNA level compared to control scrambled siRNA (siScr) transfected cells (Fig. 7A,C). As a control, we showed that under the same conditions the levels of *AXIN2* mRNA, a well-known downstream target of β -catenin, was induced (Fig. 7B,D). It has previously been shown that *FOXD3* overexpression in melanoma cell lines or cultured quail neural crest cells resulted in repression of *MITF* expression (Abel et al., 2013; Thomas and Erickson, 2009). In a converse experiment, we show here that siRNA-mediated *MITF* silencing in 501mel and SK28 human melanoma cells led to upregulation of *FOXD3* (Fig. 7E-H).

ChIP-seq in 501mel cells revealed that MITF occupied several sites at the *FOXD3* locus in a putative distal enhancer. There are at least four MITF bound sites (1-4) in 501Mel cells that are evident in this region (Fig. 7I). We focused on site 4 for several reasons. The MITF site is occupied in melanocytes, it is adjacent to a SOX10 bound site, it is associated with strong occupancy of BRG1 and H2AZ and marking by H3K27ac. All of these are hallmarks of active enhancer elements of melanoma cells. The requirement for SOX10 as a mark of the most functionally relevant sites was previously described (Laurette et al., 2015) and has been recently highlighted by others studies (Wouters et al., 2020). Nevertheless, MITF site 1 is also occupied in melanocytes and is associated with H3K27ac, but shows much lower BRG1 and H2AZ occupancy. Sites 2 and 3 are not occupied in melanocytes and show weak or no H3K27ac. We also note that sites 5-7 have all of the characteristics of regulatory elements with clear nucleosome depleted regions. At each site, a consensus E-box sequence was present along with a SOX10-binding motif at the distal enhancer. In primary human melanocytes, MITF ChIP-seq reveals a site in the proximal *FOXD3* (site 8). (Webster et al., 2014). Finally, these binding sequences were present at the otherwise well-conserved syntenic regions at the mouse *Foxd3* locus (Fig. 7I). Moreover, it is well accepted that H3K27ac is a mark of active enhancer elements and BRG1 on the other hand can also be associated with negative regulation (Laurette et al., 2015). *FoxD3* is not the only gene that is repressed by MITF. Indeed, numerous examples of genes (*PTEN*, *CDH1*, *GATA6*) are repressed by MITF (Berico et al.; Dilshat et al., 2021; Hamm et al., 2021).

Taken together, these observations suggested the presence of a reciprocal regulatory feedback loop in the melanocytic lineage where *FOXD3* repress *MITF* and *MITF* repress *FOXD3*. Since the level of *MITF* expression and activity depends on numerous factors in the melanocytic lineage, this equilibrium may be rapidly shifted in favor of *MITF* when one of these molecular pathways, such as *Wnt*/ β -catenin, is induced leading to decreased *FOXD3* levels and altered cell fate (Fig. 8).

DISCUSSION

Here, we show that a constitutively active form of β -catenin (β cat Δ ex3) differentially affects melanoblast development in the trunk and paws. In the trunk region, expression of β cat Δ ex3 did not induce any major defects in developing melanoblasts, whereas it induced strong palmo-plantar hyperpigmentation of the paws. This hyperpigmentation was due to the abnormal presence of melanocytes derived from the second wave of melanoblasts. Melanoblasts migrating in the palms and soles of the mutant mice were seen as early as E14.5, whereas they were mostly absent in WT mice. These results show that once specified, β cat Δ ex3 does not influence the development of melanoblast of the first wave, but

instead controls SCP cell-fate decisions between glial and melanocyte lineages in the ventral migratory pathway. Such difference could be due to a differential regulation of the endogenous Wnt signalling pathway in these two different environments. According to these results, the contribution of SCPs to melanocytes in the adult appeared to be restricted to the limbs.

It has been shown that Schwann cells and melanocytes are very close for several reasons besides the fact that they are derived from the neural crest. It has been shown that human melanocytes can transdifferentiate in Schwann cells (Chi et al., 2011) Spindle cell melanoma and pigmented neurofibroma possess cells with melanocyte and Schwann cell characteristics, with cells producing weakly Mitf and Tyrosinase. It gives to these cells the potential opportunity to perform a bidirectional differentiation (Motoi et al., 2005; Winnepenninckx et al., 2003). Melanotic schwannoma, a rare variant of nerve sheath tumors that arise from spinal nerve roots, is composed of neoplastic Schwann cells that produce melanin (Alexiev et al., 2018). However, the molecular status of these cells were not described but we may hypothesize that they produce Tyrosinase and therefore Mitf. Moreover, Tyrosinase promoter activity was detected in other cells than melanocytes such as the cortex, olfactory system, hippocampus, epithalamus and substantia nigra during embryonic development (Tief et al., 1998). Finally, adult melanocytes, expressing Tyrosinase, were present in many tissue/organ that was not initially suspected (see for instance review, (Brito and Kos, 2008; Colombo et al., 2011; Gudjohnsen et al., 2015; Yajima and Larue, 2008)).

Hyperpigmentation of the paws

Hyperpigmentation of the palms and soles was already described in humans and mice after cell non-autonomous induction. Human palmoplantar fibroblasts express the Wnt/ β -catenin signaling inhibitor DKK1, which inhibits melanocyte function and growth by regulating β -catenin (Yamaguchi et al., 2004; Yamaguchi et al., 2008). Downregulation of β -catenin leads to the inhibition of Mitf-M expression, and of its downstream target Tyrosinase, the key enzyme of melanogenesis. Increasing β -catenin levels in SCP-derived melanocytes may counteract the effects of Dkk1 in palmoplantar skin, promoting melanocyte differentiation after inducing Mitf and Tyrosinase. Overexpression of Kitl (Steel factor) in the basal layer of the epidermis in mice induces palmoplantar hyperpigmentation (Kunisada et al., 1998). The authors found melanoblasts in the footpads of E16.5 mutant embryos, whereas they were not present in WT littermates. As Kit signaling is involved in melanoblast migration, they proposed that increased Kit signals promote migration of melanoblasts throughout the entire paw epithelium. This explanation is certainly valid. However, Kit signaling in melanocytes

indirectly regulates β -catenin, through the PI3K pathway, and Mitf-M, through the MAPK pathway. Thus, in keeping with the results obtained here, an alternative and/or complementary explanation for the palmoplantar hyperpigmentation is enhanced melanoblast specification from SCPs. Other mutations lead to hyperpigmentation not only of the paws but also in pinna, tails of adult mice and in hair-bearing skin. A series of mutants are associated with GPCR such as Gnaq (Dsk1 – V179M, and Dsk10 – F335L) and Gna11 (Dsk7 – I63V). Gnaq and Gna11 are the main mediators of EndrB, a key regulator of melanocyte proliferation and survival (Jain et al., 2020; Van Raamsdonk et al., 2004). Another series of mutants is associated with p53, Kitl and Kit; Rps19 (Dsk3 – T316A/Y54N) and Rps20 (Dsk4 – T29C/L32P and T2201A in 3' UTR). Interestingly, heterozygous Rps19 or Rps20 mutation in keratinocyte activate p53 that induces the level of Kitl to induce Kit present at the surface of melanocytes (McGowan et al., 2008).

Specification

As previously mentioned, β -catenin is involved in cell-fate specification, a process involving complex combinations of cell intrinsic and extracellular signals that need to be correctly delivered in time and space. The role of β -catenin in the specification of first wave melanocytes has been clearly demonstrated. The high level of β -catenin in premigratory neural crest cells promote the expansion and differentiation of mouse melanoblasts as it was shown *in vitro* by Dunn and colleagues after infecting neural tube with RCAS-Wnt1 retrovirus (Dunn et al., 2000) or *in vivo* by Hari and colleagues after inducing β -catenin using the Wnt1-Cre mice (Hari et al., 2002). In both cases, the high level of β -catenin induces M-Mitf, and induces Tyr, at a time that some cells are not yet determined. In both cases, Wnt1 is produced in premigratory neural crest cells, but Tyrosinase is not. In consequence, using the Tyr::CreERT2 with an early tamoxifen induction or Tyr::Cre mice, the expansion and differentiation of mouse melanoblasts from premigratory neural crest cells would not be possible, since Cre or CreERT2 is not present in these cells; the promotion of the first wave of melanoblast may not occur. It is also important to remind that it remains unknown if CreERT2 is produced at E8.5. Using Wnt1::Cre or Tyr::Cre mice to delete the exon 3 of β -catenin, melanocytes were present at higher level than normal in various part of the body including sympathetic ganglia, spleen, heart and brain (Yajima et al., 2013). However, using Tyr::CreERT2 with a tamoxifen induction at E10.5, we did not observe melanocytes at ectopic sites other than the palms. The inactivation of β -catenin in NCC prior to melanoblast specification using Wnt1::Cre shows that β -catenin is essential for the generation of melanoblasts. The absence of β -catenin apparently does not impair early SCP specification, as specific markers are produced (Hari et al., 2002). Thus, SCPs and second wave

melanocytes still form in these animals. This series of experiments showed the critical function of Wnt signaling in driving early melanoblast specification and could explain the absence of first-wave melanocytes (*i.e.* migrating dorso-laterally), but the importance of β -catenin in the generation of second wave melanocytes was still unknown. As Schwann cells and second wave melanocytes share a common SCP precursor, we hypothesized that β -catenin in the β cat Δ ex3 mutant mice is activated in SCPs that migrate via the ventral pathway, altering their fate and promoting their differentiation into melanocytes. Whereas neural progenitors and glial cells express the Foxd3 transcription factor, it is not expressed in melanoblasts (Kos et al., 2001). As Mitf is the key transcription factor specifying the melanocyte lineage and knowing that SCPs express Foxd3, Mitf and Sox10, it is likely that SCP fate is governed by the relative amounts/activities of Foxd3 and Mitf. In agreement with this hypothesis, constitutive activation of β -catenin in Schwannoma cells led to FOXD3 repression, whereas *MITF* silencing up-regulated FOXD3 expression in melanoma cell lines. Moreover, MITF binds to regulatory elements at the *FOXD3* locus in human melanoma cells and primary melanocytes and may therefore directly inhibits its expression. In contrast, overexpression of FOXD3 in melanoma cell lines represses *MITF* expression (Abel et al., 2013; Thomas and Erickson, 2009). Together these observations support the idea that a direct and reciprocal negative regulation of FOXD3 and MITF expression can affect SCP fate. This model is reminiscent of the reciprocal negative regulation seen with MITF and JUN that affects the phenotype switch between melanocytic and undifferentiated melanoma cell states (Riesenberg et al., 2015). Based on these observations, we propose that high β -catenin levels in SCP at the time of their specification increases *Mitf* expression, hence repressing *FoxD3* expression and enhancing melanocyte specification at the expense of glia. At this point, we cannot exclude that β -catenin might repress *FoxD3* expression through other pathways. Such a model is supported by the reduced numbers of Gfap-positive cells and increased numbers of Mitf-positive or Dct-positive cells observed in the paws of β cat Δ ex3 mice, suggesting that a cell fate switch occurred.

Acral melanoma

Although the number of melanocytes in the soles of the feet and palms of the hands are very limited, these cells may transform in acral melanoma (ALM). ALM and nodular melanoma (NM) are more aggressive than superficial spreading melanoma (SSM). The percentage of ALM is higher in Asians (50%) than in Caucasians (10%). This is because NM and SSM are very rare in Asians, but the risk to develop an ALM appears to be similar between Asians and Caucasians. At the molecular level, the main mutations in ALM and non-ALM are similar; they include mutations in the *BRAF*, *NRAS*, *NF1*, and *KIT* genes, but the proportions are different (Moon et al., 2018; Zebary et al., 2013). NM and SSM arise from melanocytes

determined from the first wave of melanoblasts, one could speculate that ALM could arise from melanocytes derived from the second wave of melanoblasts. This hypothesis has to be put in perspective with a recent work showing that ALM may emerge from McSC located in sweat glands (Eshiba et al., 2021). While sun exposure is a well-established cause for melanoma development, the soles and palms are non-sun-exposed regions, raising the issue of the importance of the embryonic origin of melanocytes in melanomagenesis and how this may influence their aggressivity when transformed.

Conclusion

β -catenin appears to play a complex role in the melanocyte lineage, depending on tight regulation of its levels and time and place of induction. We show here that expression of β cat Δ ex3 after specification of the melanoblasts of the first wave in Tyr::Cre- and Tyr::CreER^{T2}-expressing cells does not appear to affect melanoblast development in the dorso-lateral pathway, but favors melanoblast specification in the ventral pathway.

MATERIALS AND METHODS

Transgenic mouse generation and genotyping

Animal care, use, and experimental procedures were conducted in accordance with recommendations of the European Community (86/609/EEC) and Union (2010/63/UE) and the French National Committee (87/848). Animal care and use were approved by the ethics committee of the Curie Institute in compliance with the institutional guidelines.

Mice with conditional constitutive stabilization of β -catenin were generated by mating Tyr::CreA and Tyr::Cre-ER^{T2-Lar} (designated in the text as Tyr::Cre-ER^{T2}) transgenic mice (Delmas et al., 2003; Yajima et al., 2006) with animals homozygous for a floxed allele of β -catenin, with LoxP sites flanking exon 3 (Δ ex3) (Harada et al., 1999). Z/EG mice were used to follow defloxed cells (Novak et al., 2000). Transgenic mice were maintained on a pure C57BL/6J background (backcrossed at least 10 times). All animals were housed in specific pathogen-free conditions in the animal facility. Mice were genotyped using DNA isolated from tail biopsies using standard PCR conditions. The Tyr::Cre transgene (0.4 kb fragment) was detected by PCR, as previously described (Delmas et al., 2003). For detection of the floxed (570bp) and WT (376bp) alleles of the β -catenin gene, PCR amplification was carried out with the forward primer (LL523) 5'-GAC ACC GCT GCG TGG ACA ATG-3' and the reverse primer (LL524) 5'-GTG GCT GAC AGC AGC TTT TCT G-3'. The forward primer (LL667) 5'-CGT GGA CAA TGG CTA CTC A-3' and the reverse primer (LL668) 5'-CTG AGC CCT AGT CAT TGC AT-3' were used for detection of the WT (715bp) and deleted (450bp) alleles of the

β -catenin gene. The PCR conditions were as follows: 5 min at 94°C followed by 35 cycles of 20 s at 94°C, 30 s at 56.5°C, 45 s at 72°C, and a final extension of 10 min at 72°C.

Tamoxifen injection

Pregnant C57BL/6J mice were injected intraperitoneally at E8.5, E10.5 or E11.5 with tamoxifen (Sigma) diluted in corn oil. An amount of 0.5mg of tamoxifen was injected for 20g of body weight. This dose of tamoxifen was not optimal but higher doses induced embryonic death and resorption of the embryos.

Histology

Mice were crossed with Dct::LacZ (MacKenzie et al., 1997) and the resulting embryos collected at various times during pregnancy. Embryos were stained with X-gal, as previously described (Delmas et al., 2003). Paws of new-born mice at P1 were dissected, washed in PBS, and fixed by incubation in 0.25% glutaraldehyde in PBS for 50 min at 4°C. They were then incubated in 30% sucrose/PBS overnight, followed by 30% sucrose/50% OCT/PBS for 5h and embedded in Optimal Cacodylate Compound (OCT). Cryosections (7 μ m thick) were stained either with heamatoxylin and eosin or X-gal as follows: they were washed twice in PBS at 4°C, and incubated twice, for 10 min, in permeabilization solution (0.1M phosphate buffer pH7.3, 2mM MgCl₂, 0.01% sodium deoxycholate, 0.02% NP-40) at room temperature. They were then incubated in staining solution (0.4mg/mL 5-bromo-4-chloro-3-indolyl-D-galactosidase, 2 mM potassium ferricyanide, 2 mM potassium ferrocyanide, 4 mM MgCl₂, 0.01% sodium deoxycholate, and 0.02% NP-40 in PBS) overnight at 30°C. Sections were post-fixed in 4% PFA overnight at 4°C, washed in PBS, and stained with eosin. Paws of newborn mice at P5 were fixed in 4% PFA, dehydrated, and embedded in paraffin by standard methods. Paraffin sections (7 μ m thick) were stained with eosin.

Immunostaining

Embryos were collected at various stages of development. Embryos and/or skins dissected from the back of the mice were washed in PBS and fixed by overnight incubation in 4% PFA. They were then either incubated in 30% sucrose/PBS overnight, followed by 30% sucrose/50% OCT/PBS for 5 h and embedded in OCT, or dehydrated and embedded in paraffin. Sections (7 μ m thick) were washed with PBS-Tween 0.1% (PBT) for 10 min. Antigens were then retrieved by incubation for 20 min in citric acid buffer (pH 7.4) at 90°C. Non-specific binding was blocked by incubation with 2% skimmed milk powder in PBT. Sections were incubated overnight at 4°C with various primary antibodies. Rabbit polyclonal antibody against β -catenin (Abcam ab6302, dilution 1/1,000), chicken polyclonal antibody against β -galactosidase (Abcam ab9361, dilution 1/400), mouse monoclonal antibody against

Tubulin β 3 (clone TUJ1, BioLegend 801213, dilution 1/200), rabbit monoclonal antibody against gp100/Pmel (Abcam ab137078, dilution 1/300) were used. Sections were washed three times in PBST for 5 min each and incubated with secondary antibodies for 1h at 37°C. The secondary antibodies used were donkey Alexa 488-anti-rabbit, donkey Alexa 555-anti-chicken, donkey Alexa 488-anti-mouse and donkey Alexa 555-anti-rabbit (Molecular Probes) each at a dilution of 1/500. Sections were incubated in DAPI for 10 min, washed three times in PBT, for 10 min each, and mounted in mounting media containing N-propylgalate. Conventional fluorescence photomicrographs were obtained with a Leica DM IRB inverted routine microscope.

Whole mount immunostaining

E13.5 and E15.5 embryos paws were collected and fixed in 4% PFA-PBS pH7.5 (Euromedex) for 6 hours prior washing them three times in PBT. Paws were dehydrated in a series of PBS/methanol incubation (25%, 50%, 75% and 100%) for 10min each. Paws were incubated 24 hours in methanol at 4°C prior bleaching them for 24h in a mixture of 1/3 H₂O₂ and 2/3 methanol 30%. Paws were washed three times in methanol prior post-fixed them overnight in 1/5 DMSO and 4/5 pure methanol. Paws were sequentially rehydrated in PBS/methanol (75%, 50%, 25% and 0%) for 10 min each prior washing them twice in PBT. Paws were incubated overnight at room temperature in PBS containing 5% Donkey serum, 1% BSA and 20% DMSO as blocking solution. After blocking, paws were incubated with primary antibody(ies) in the blocking solution at 1/1,000 for five days at RT. Primary antibodies were rabbit against neurofilament (Abcam ab9034), mouse against Gfap (Sigma C9205 & Cell Signalling Technology 3670) and goat against Mitf (R&D system AF5769). Secondary antibodies were diluted in the blocking solution: alexaFluor 555 (Invitrogen A-31572), alexaFluor488 (Invitrogen A21202) and alexaFluor633 (Invitrogen A-21082) for overnight at RT at dilution 1/1,000. Staining was ended after incubation of the paws in Dapi for 4 hours at RT. Embryos were dehydrated in PBS/methanol (25%, 50%, 75% and 100%) for 10min each at RT. Chambers made by 1mm thick Fastwell (Sigma) coated on a glass slide was used to incorporate the paws. Each paw was fixed on to the glass slide with 1% NuSieve Agarose (Sigma) and covered with methanol. After three washes with methanol, paws were incubated twice for 5min with methanol 50% BABB (1/3 benzylalcohol and 2/3 benzylbenzoate, from Sigma), and then three times in pure BABB for 5min each (or until the sample is cleared). The chamber was closed with coverslip and sealed with nail polish prior examination under the microscope.

Confocal imaging and ImageJ treatment for 3D reconstruction

Z-sections were acquired every 5µm for the dorsal and ventral part of the limb with a Confocal Leica SP5 microscope. Then, the plugin PureDenoise was used on the stack to increase the signal, and finally the filter substrate background (20) was used to remove the remaining background. 3D reconstructions were performed from stacks containing the same number of sections and the same biological structures in WT and mutants, using 3D project in *ImageJ* without interpolation.

BrdU labelling

Melanocyte proliferations were analyzed using BrdU labelling *in vivo* on embryos at various stages of development. BrdU (100 µg/mL, BD Biosciences) was injected intra-peritoneally into the pregnant mother 2 h before sacrifice, in the form of two 50-µg/mL injections administered at 20-min intervals. Embryos were collected for immunohistochemistry. They were fixed and stained, as described above, with mouse monoclonal anti-BrdU antibody (BD Biosciences 555627, dilution 1/200) and chicken polyclonal anti-β-galactosidase antibody (Abcam ab9361, dilution 1/400). Donkey Alexa 488-anti-mouse and donkey Alexa 555-anti-chicken (Molecular Probes) were used as secondary antibodies each at a dilution of 1/500.

Melanoblast counts on the paws

Pictures of Xgal stained paws were taken using a binocular magnifying glass with a 1x objective. Proximal area (from the body to the migrating front, between the dotted yellow and black lines) and distal area (after the black dotted line) were delimited on the picture. Blue dots (melanoblasts) were counted using *ImageJ* software. At least 5 embryos were counted for each genotype at each stage in both areas.

Cell culture and siRNA-mediated knockdown

501mel and SK28 human melanoma cell lines were grown in RPMI 1640 media (GIBCO) supplemented with 10% FCS (GIBCO) and 1% Penicillin-Streptomycin (GIBCO) (Rambow et al., 2015). HEI-193 Schwannoma and IPN 2.03 Schwann cells were grown in DMEM media (GIBCO) supplemented with 10% FCS (GIBCO) and 1% Penicillin-Streptomycin (GIBCO) (Fraenzer et al., 2003; Li et al., 2016). Cells were maintained at 37°C in a humidified atmosphere containing 5% CO₂. Cells are routinely tested for the absence of mycoplasmas using MycoAlert (Lonza). siRNA targeting human MITF (M-008674) and APC (L-003869) were purchased from Dharmacon. Si Scramble (siSCR), with no known human targets, was purchased from Eurofins Genomics. Cells were transfected with 100pmol siRNA or siScr with Lipofectamine2000 (Invitrogen) and assayed for mRNA expression 48h post-transfection.

RNA extraction and RT-qPCR

Total RNA was extracted from cell lines using the miRNeasy kit (Qiagen). M-MLV reverse transcriptase (Invitrogen) was used according to the manufacturer's protocol to synthesize cDNA from 1 µg total RNA in combination with random hexamers. Quantitative RT-PCR was performed with the iTaq universal Sybrgreen Supermix (BIORAD) and primers listed below, using a QuantStudio 5 thermocycler (Applied Biosystem) in a final reaction volume of 25 µL under the following conditions: 95°C for 1.5min, 40 cycles of 95°C for 30s, 60°C for 60s, with a final melting curve analysis. Relative expression was determined by the comparative $\Delta\Delta C_t$ method. PCR primers: FOXD3 f: 5'-CAT CCG CCA CAA CCT CTC-3'; FOXD3 r: 5'-CAT ATG AGC GCC GTC TG-3'; MITF f: 5'-CTA TGC TTA CGC TTA ACT CCA-3'; MITF r: 5'-TAC ATC ATC CAT CTG CAT ACA G-3'; AXIN2 f: 5'-CCT AAA GGT CGT GTG TGG CT-3'; AXIN2 r: 5'-GTG CAA AGA CAT AGC CAG AAC C-3'; TBP f: 5'-CAC GAA CCA CGG CAC TGA TT-3'; TBP r: 5'-TTT TCT TGC TGC CAG TCT GGA C-3'.

Statistical analysis

Statistical tests are detailed in the figure legends. Data are presented as mean \pm SEM. Statistical analyses were performed with Prism 5 software (GraphPad).

ACKNOWLEDGEMENTS

We are grateful to Dominique Lallemand and Eric Pasmant for providing HEI-193 and IPN 02.3 cell lines. We thank the teams caring for the imaging, histology and animal colony facilities of the Institut Curie, especially Pauline Dubreuil and Mirella Miranda.

FUNDING

This work was supported by the Ligue Contre le Cancer, Fondation ARC, and is under the program «Investissements d'Avenir» launched by the French Government and implemented by ANR Labex CelTisPhyBio (ANR-11-LBX-0038 and ANR-10-IDEX-0001-02 PSL). S.C. was supported by fellowships from MENRT and FRM. R.Y.W. was supported by fellowships from MENRT and ARC.

CONFLICT OF INTEREST

S.C. serves a consultant for Q-State Biosciences, Inc. All other authors declare no conflict of interest.

REFERENCES

- Abel, E. V., Basile, K. J., Kugel, C. H., 3rd, Witkiewicz, A. K., Le, K., Amaravadi, R. K., Karakousis, G. C., Xu, X., Xu, W., Schuchter, L. M., et al. (2013). Melanoma adapts to RAF/MEK inhibitors through FOXD3-mediated upregulation of ERBB3. *J Clin Invest* **123**, 2155-2168.
- Adameyko, I. and Lallemand, F. (2010). Glial versus melanocyte cell fate choice: Schwann cell precursors as a cellular origin of melanocytes. *Cellular and molecular life sciences : CMLS* **67**, 3037-3055.
- Adameyko, I., Lallemand, F., Aquino, J. B., Pereira, J. A., Topilko, P., Muller, T., Fritz, N., Beljajeva, A., Mochii, M., Liste, I., et al. (2009). Schwann cell precursors from nerve innervation are a cellular origin of melanocytes in skin. *Cell* **139**, 366-379.
- Adameyko, I., Lallemand, F., Furlan, A., Zinin, N., Aranda, S., Kitambi, S. S., Blanchart, A., Favaro, R., Nicolis, S., Lubke, M., et al. (2012). Sox2 and Mitf cross-regulatory interactions consolidate progenitor and melanocyte lineages in the cranial neural crest. *Development* **139**, 397-410.
- Aktary, Z., Bertrand, J. U. and Larue, L. (2016). The WNT-less wonder: WNT-independent beta-catenin signaling. *Pigment cell & melanoma research*.
- Alexiev, B. A., Chou, P. M. and Jennings, L. J. (2018). Pathology of Melanotic Schwannoma. *Arch Pathol Lab Med* **142**, 1517-1523.
- Berico, P., Cigrang, M., Davidson, G., Braun, C., Sandoz, J., Legras, S., Vokshi, B. H., Slovic, N., Peyresaubes, F., Gene Robles, C. M., et al. (2021). CDK7 and MITF repress a transcription program involved in survival and drug tolerance in melanoma. *EMBO Rep.* **22**, e51683.
- Brito, F. C. and Kos, L. (2008). Timeline and distribution of melanocyte precursors in the mouse heart. *Pigment cell & melanoma research* **21**, 464-470.
- Carreira, S., Goodall, J., Denat, L., Rodriguez, M., Nuciforo, P., Hoek, K. S., Testori, A., Larue, L. and Goding, C. R. (2006). Mitf regulation of Dia1 controls melanoma proliferation and invasiveness. *Genes Dev* **20**, 3426-3439.
- Chi, G. F., Kim, D. W., Jiang, M. H., Yoon, K. J. and Son, Y. (2011). Schwann-like cells from human melanocytes and their fate in sciatic nerve injury. *Neuroreport* **22**, 603-608.
- Colombo, S., Berlin, I., Delmas, V. and Larue, L. (2011). Classical and non-classical melanocytes in vertebrates. In *Melanins and melanosomes* (ed. P. A. Riley & J. Borovansky), pp. 21-51. Weinheim: Wiley-VCH Verlag & Co.
- Curran, K., Raible, D. W. and Lister, J. A. (2009). Foxd3 controls melanophore specification in the zebrafish neural crest by regulation of Mitf. *Dev Biol* **332**, 408-417.
- Delmas, V., Martinozzi, S., Bourgeois, Y., Holzenberger, M. and Larue, L. (2003). Cre-mediated recombination in the skin melanocyte lineage. *Genesis* **36**, 73-80.

- Dilshat, R., Fock, V., Kenny, C., Gerritsen, I., Lasseur, R. M. J., Travnickova, J., Eichhoff, O., Cerny, P., Möller, K., Sigurbjörnsdóttir, S., et al. (2021). MITF reprograms the extracellular matrix and focal adhesion in melanoma. *Elife*, 10:e63093.
- Dorsky, R. I., Moon, R. T. and Raible, D. W. (1998). Control of neural crest cell fate by the Wnt signalling pathway. *Nature* **396**, 370-373.
- Dunn, K. J., Williams, B. O., Li, Y. and Pavan, W. J. (2000). Neural crest-directed gene transfer demonstrates Wnt1 role in melanocyte expansion and differentiation during mouse development. *Proc Natl Acad Sci U S A* **97**, 10050-10055.
- Dupin, E., Glavieux, C., Vaigot, P. and Le Douarin, N. M. (2000). Endothelin 3 induces the reversion of melanocytes to glia through a neural crest-derived glial-melanocytic progenitor. *Proc Natl Acad Sci U S A* **97**, 7882-7887.
- Dupin, E., Real, C., Glavieux-Pardanaud, C., Vaigot, P. and Le Douarin, N. M. (2003). Reversal of developmental restrictions in neural crest lineages: transition from Schwann cells to glial-melanocytic precursors in vitro. *Proc Natl Acad Sci U S A* **100**, 5229-5233.
- Eshiba, S., Namiki, T., Mohri, Y., Aida, T., Serizawa, N., Shibata, T., Morinaga, H., Nanba, D., Hiraoka, Y., Tanaka, K., et al. (2021). Stem cell spreading dynamics intrinsically differentiate acral melanomas from nevi. *Cell Reports* **36**, 109492.
- Fraenzer, J. T., Pan, H., Minimo, L. J., Smith, G. M., Knauer, D. and Hung, G. (2003). Overexpression of the NF2 gene inhibits schwannoma cell proliferation through promoting PDGFR degradation. *Int J Oncol.* **23**, 1493-1500.
- Furlan, A. and Adameyko, I. (2018). Schwann cell precursor: a neural crest cell in disguise? *Dev Biol* **444 Suppl 1**, S25-S35.
- Gat, U., DasGupta, R., Degenstein, L. and Fuchs, E. (1998). De Novo hair follicle morphogenesis and hair tumors in mice expressing a truncated beta-catenin in skin. *Cell* **95**, 605-614.
- Gudjohnsen, S. A., Atacho, D. A., Gesbert, F., Raposo, G., Hurbain, I., Larue, L., Steingrimsson, E. and Petersen, P. H. (2015). Meningeal Melanocytes in the Mouse: Distribution and Dependence on. *Front Neuroanat* **9**, 149.
- Hamm, M., Sohler, P., Petit, V., Raymond, J. H., Delmas, V., Le Coz, M., Gesbert, F., Kenny, C., Aktary, Z., Pouteaux, M., et al. (2021). BRN2 is a non-canonical melanoma tumor-suppressor. *Nat Commun.* **12**, 3707.
- Harada, N., Tamai, Y., Ishikawa, T., Sauer, B., Takaku, K., Oshima, M. and Taketo, M. M. (1999). Intestinal polyposis in mice with a dominant stable mutation of the beta-catenin gene. *Embo J* **18**, 5931-5942.
- Hari, L., Brault, V., Kleber, M., Lee, H. Y., Ille, F., Leimeroth, R., Paratore, C., Suter, U., Kemler, R. and Sommer, L. (2002). Lineage-specific requirements of beta-catenin in neural crest development. *J Cell Biol* **159**, 867-880.
- Hari, L., Miescher, I., Shakhova, O., Suter, U., Chin, L., Taketo, M., Richardson, W. D., Kessar, N. and Sommer, L. (2012). Temporal control of neural crest lineage generation by Wnt/beta-catenin signaling. *Development* **139**, 2107-2117.

- Hirobe, T.** (1984). Histochemical survey of the distribution of the epidermal melanoblasts and melanocytes in the mouse during fetal and postnatal periods. *Anat Rec* **208**, 589-594.
- Hornyak, T. J., Hayes, D. J., Chiu, L. Y. and Ziff, E. B.** (2001). Transcription factors in melanocyte development: distinct roles for Pax-3 and Mitf. *Mech Dev* **101**, 47-59.
- Ikeya, M., Lee, S. M., Johnson, J. E., McMahon, A. P. and Takada, S.** (1997). Wnt signalling required for expansion of neural crest and CNS progenitors. *Nature* **389**, 966-970.
- Imbert, A., Eelkema, R., Jordan, S., Feiner, H. and Cowin, P.** (2001). Delta N89 beta-catenin induces precocious development, differentiation, and neoplasia in mammary gland. *J Cell Biol* **153**, 555-568.
- Jacob, C.** (2015). Transcriptional control of neural crest specification into peripheral glia. *Glia*.
- Jain, F., Longakit, A., Huang, J. L. and Van Raamsdonk, C. D.** (2020). Endothelin signaling promotes melanoma tumorigenesis driven by constitutively active GNAQ. *Pigment Cell Melanoma Res.* **33**, 834-849.
- Kinsler, V. A. and Larue, L.** (2018). The patterns of birthmarks suggest a novel population of melanocyte precursors arising around the time of gastrulation. *Pigment cell & melanoma research* **31**, 95-109.
- Kos, R., Reedy, M. V., Johnson, R. L. and Erickson, C. A.** (2001). The winged-helix transcription factor FoxD3 is important for establishing the neural crest lineage and repressing melanogenesis in avian embryos. *Development* **128**, 1467-1479.
- Kunisada, T., Yoshida, H., Yamazaki, H., Miyamoto, A., Hemmi, H., Nishimura, E., Shultz, L. D., Nishikawa, S. and Hayashi, S.** (1998). Transgene expression of steel factor in the basal layer of epidermis promotes survival, proliferation, differentiation and migration of melanocyte precursors. *Development* **125**, 2915-2923.
- Laurette, P., Strub, T., Koludrovic, D., Keime, C., Le Gras, S., Seberg, H., Van Otterloo, E., Imrichova, H., Siddaway, R., Aerts, S., et al.** (2015). Transcription factor MITF and remodeler BRG1 define chromatin organisation at regulatory elements in melanoma cells. *Elife* **4**.
- Le Douarin, N. and Kalcheim, C.** (1999). *The neural crest* (Second edition edn). Cambridge: Cambridge University Press.
- Lee, H. Y., Kleber, M., Hari, L., Brault, V., Suter, U., Taketo, M. M., Kemler, R. and Sommer, L.** (2004). Instructive role of Wnt/beta-catenin in sensory fate specification in neural crest stem cells. *Science* **303**, 1020-1023.
- Li, H., Chang, L. J., Neubauer, D. R., Muir, D. F. and Wallace, M. R.** (2016). immortalization of human normal and NF1 neurofibroma Schwann cells. *Lab Invest.* **96**, 1105-1115.
- Luciani, F., Champeval, D., Herbette, A., Denat, L., Aylaj, B., Martinuzzi, S., Ballotti, R., Kemler, R., Goding, C. R., De Vuyst, F., et al.** (2011). Biological and mathematical modeling of melanocyte development. *Development* **138**, 3943-3954.

- MacKenzie, M. A., Jordan, S. A., Budd, P. S. and Jackson, I. J.** (1997). Activation of the receptor tyrosine kinase Kit is required for the proliferation of melanoblasts in the mouse embryo. *Dev Biol* **192**, 99-107.
- McGowan, K. A., Li, J. Z., Park, C. Y., Beaudry, V., Tabor, H. K., Sabnis, A. J., Zhang, W., Fuchs, H., Hrabe de Angelis, M., Myers, R. M., et al.** (2008). Ribosomal mutations cause p53-mediated dark skin and pleiotropic effects. *Nature Genetics* **40**, 963-970.
- Moon, K. R., Choi, Y. D., Kim, J. M., Jin, S., Shin, M. H., Shim, H. J., Lee, J. B. and Yun, S. J.** (2018). Genetic Alterations in Primary Acral Melanoma and Acral Melanocytic Nevus in Korea: Common Mutated Genes Show Distinct Cytomorphological Features. *The Journal of investigative dermatology* **138**, 933-945.
- Motoi, T., Ishida, T., Kawato, A., Motoi, N. and Fukayama, M.** (2005). Pigmented neurofibroma: review of Japanese patients with an analysis of melanogenesis demonstrating coexpression of c-met protooncogene and microphthalmia-associated transcription factor. *Hum Pathol.* **36**, 871-877.
- Nitzan, E., Krispin, S., Pfaltzgraff, E. R., Klar, A., Labosky, P. A. and Kalcheim, C.** (2013a). A dynamic code of dorsal neural tube genes regulates the segregation between neurogenic and melanogenic neural crest cells. *Development* **140**, 2269-2279.
- Nitzan, E., Pfaltzgraff, E. R., Labosky, P. A. and Kalcheim, C.** (2013b). Neural crest and Schwann cell progenitor-derived melanocytes are two spatially segregated populations similarly regulated by Foxd3. *Proceedings of the National Academy of Sciences of the United States of America* **110**, 12709-12714.
- Novak, A., Guo, C., Yang, W., Nagy, A. and Lobe, C. G.** (2000). Z/EG, a double reporter mouse line that expresses enhanced green fluorescent protein upon Cre-mediated excision. *Genesis* **28**, 147-155.
- Petit, V. and Larue, L.** (2016). Any route for melanoblasts to colonize the skin! *Exp Dermatol.*
- Puig, I., Champeval, D., De Santa Barbara, P., Jaubert, F., Lyonnet, S. and Larue, L.** (2009). Deletion of Pten in the mouse enteric nervous system induces ganglioneuromatosis and mimics intestinal pseudoobstruction. *J Clin Invest* **119**, 3586-3596.
- Radu, A. G., Torch, S., Fauvelle, F., Pernet-Gallay, K., Lucas, A., Blervaque, R., Delmas, V., Schlattner, U., Lafanechère, L., Hainaut, P., et al.** (2019). LKB1 specifies neural crest cell fates through pyruvate-alanine cycling. *Sci Adv.* **5**.
- Rambow, F., Job, B., Petit, V., Gesbert, F., Delmas, V., Seberg, H., Meurice, G., Van Otterloo, E., Dessen, P., Robert, C., et al.** (2015). New Functional Signatures for Understanding Melanoma Biology from Tumor Cell Lineage-Specific Analysis. *Cell Rep* **13**, 840-853.
- Real, C., Glavieux-Pardanaud, C., Le Douarin, N. M. and Dupin, E.** (2006). Clonally cultured differentiated pigment cells can dedifferentiate and generate multipotent progenitors with self-renewing potential. *Dev Biol* **300**, 656-669.

- Riesenberg, S., Groetchen, A., Siddaway, R., Bald, T., Reinhardt, J., Smorra, D., Kohlmeyer, J., Renn, M., Phung, B., Aymans, P., et al. (2015). MITF and c-Jun antagonism interconnects melanoma dedifferentiation with pro-inflammatory cytokine responsiveness and myeloid cell recruitment. *Nat Commun* **6**, 8755.
- Romagnolo, B., Berrebi, D., Saadi-Keddoucci, S., Porteu, A., Pichard, A. L., Peuchmaur, M., Vandewalle, A., Kahn, A. and Perret, C. (1999). Intestinal dysplasia and adenoma in transgenic mice after overexpression of an activated beta-catenin. *Cancer Res* **59**, 3875-3879.
- Silvers, W. K. (1979). *The coat colors of Mice*. New York: Springer-Verlag.
- Steingrimsson, E., Copeland, N. G. and Jenkins, N. A. (2004). Melanocytes and the microphthalmia transcription factor network. *Annu Rev Genet* **38**, 365-411.
- Steinhart, Z. and Angers, S. (2018). Wnt signaling in development and tissue homeostasis. *Development* **145**.
- Thomas, A. J. and Erickson, C. A. (2009). FOXD3 regulates the lineage switch between neural crest-derived glial cells and pigment cells by repressing MITF through a non-canonical mechanism. *Development* **136**, 1849-1858.
- Tief, K., Schmidt, A. and Beermann, F. (1998). New evidence for presence of tyrosinase in substantia nigra, forebrain and midbrain. *Brain Res Mol Brain Res* **53**, 307-310.
- Van Raamsdonk, C. D. and Deo, M. (2013). Links between Schwann cells and melanocytes in development and disease. *Pigment cell & melanoma research* **26**, 634-645.
- Van Raamsdonk, C. D., Fitch, K. R., Fuchs, H., Hrabé de Angelis, M. and Barsh, G. S. (2004). Effects of G-protein mutations on skin color. *Nat Genet.* **36**, 961–968.
- Webster, D. E., Barajas, B., Bussat, R. T., Yan, K. J., Neela, P. H., Flockhart, R. J., Kovalski, J., Zehnder, A. and Khavari, P. A. (2014). Enhancer-targeted genome editing selectively blocks innate resistance to onco kinase inhibition. *Genome Res* **24**, 751-760.
- Winnepenninckx, V., De Vos, R., Stas, M. and van den Oord, J. J. (2003). New phenotypical and ultrastructural findings in spindle cell (desmoplastic/neurotropic) melanoma **11**, 319-325.
- Wouters, J., Kalender-Atak, Z., Minnoye, L., Spanier, K. I., De Waegeneer, M., Bravo González-Blas, C., Mauduit, D., Davie, K., Hulselmans, G., Najem, A., et al. (2020). Robust gene expression programs underlie recurrent cell states and phenotype switching in melanoma. *Nat Cell Biol.* **22**, 986-998.
- Yajima, I., Belloir, E., Bourgeois, Y., Kumasaka, M., Delmas, V. and Larue, L. (2006). Spatiotemporal gene control by the Cre-ERT2 system in melanocytes. *Genesis* **44**, 34-43.
- Yajima, I., Colombo, S., Puig, I., Champeval, D., Kumasaka, M., Belloir, E., Bonaventure, J., Mark, M., Yamamoto, H., Taketo, M. M., et al. (2013). A subpopulation of smooth muscle cells, derived from melanocyte-competent precursors, prevents patent ductus arteriosus. *PLoS ONE* **8**, e53183.

- Yajima, I. and Larue, L.** (2008). The location of heart melanocytes is specified and the level of pigmentation in the heart may correlate with coat color. *Pigment cell & melanoma research* **21**, 471-476.
- Yamaguchi, Y., Itami, S., Watabe, H., Yasumoto, K., Abdel-Malek, Z. A., Kubo, T., Rouzaud, F., Tanemura, A., Yoshikawa, K. and Hearing, V. J.** (2004). Mesenchymal-epithelial interactions in the skin: increased expression of dickkopf1 by palmoplantar fibroblasts inhibits melanocyte growth and differentiation. *J Cell Biol* **165**, 275-285.
- Yamaguchi, Y., Passeron, T., Hoashi, T., Watabe, H., Rouzaud, F., Yasumoto, K., Hara, T., Tohyama, C., Katayama, I., Miki, T., et al.** (2008). Dickkopf 1 (DKK1) regulates skin pigmentation and thickness by affecting Wnt/beta-catenin signaling in keratinocytes. *FASEB J* **22**, 1009-1020.
- Zebary, A., Omholt, K., Vassilaki, I., Hoiom, V., Linden, D., Viberg, L., Kanter-Lewensohn, L., Johansson, C. H. and Hansson, J.** (2013). KIT, NRAS, BRAF and PTEN mutations in a sample of Swedish patients with acral lentiginous melanoma. *J Dermatol Sci* **72**, 284-289.

Figures

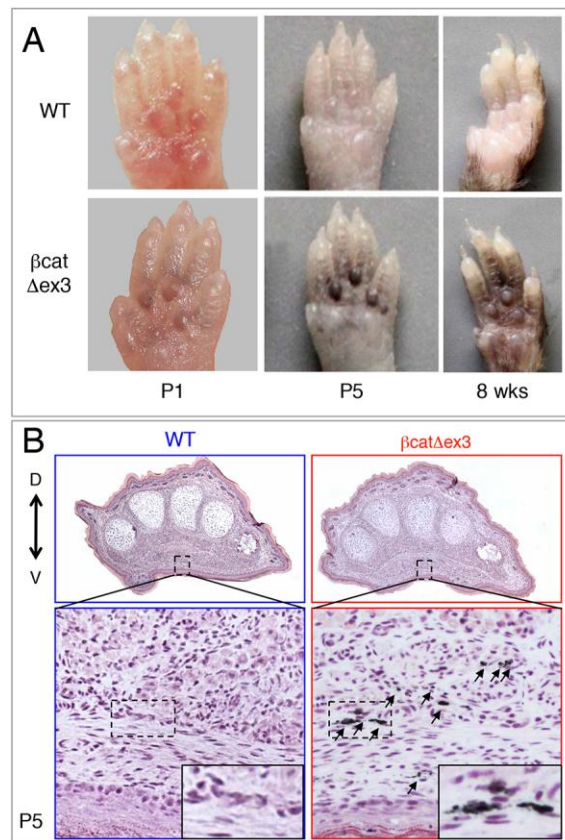


Figure 1. $\text{Tyr}::\text{Cre}^{\circ}$; $\beta\text{catex}3^{\text{flox/+}}$ mice present palmpantalar hyperpigmentation.

A) Ventral views of WT and $\beta\text{catex}3$ anterior mouse paws in newborns (P1 and P5) and adults. B) Hematoxylin and eosin staining of P5 transversal paw sections. D = dorsal. V = ventral. Arrows point to pigmented cells. WT = ($^{\circ}/^{\circ}$; $\beta\text{catex}3^{\text{flox/+}}$) or ($\text{Tyr}::\text{Cre}$; $\beta\text{catex}3^{+/+}$); $\beta\text{cat}^{\Delta\text{ex}3}$ = ($\text{Tyr}::\text{Cre}^{\circ}$; $\beta\text{catex}3^{\text{flox/+}}$).

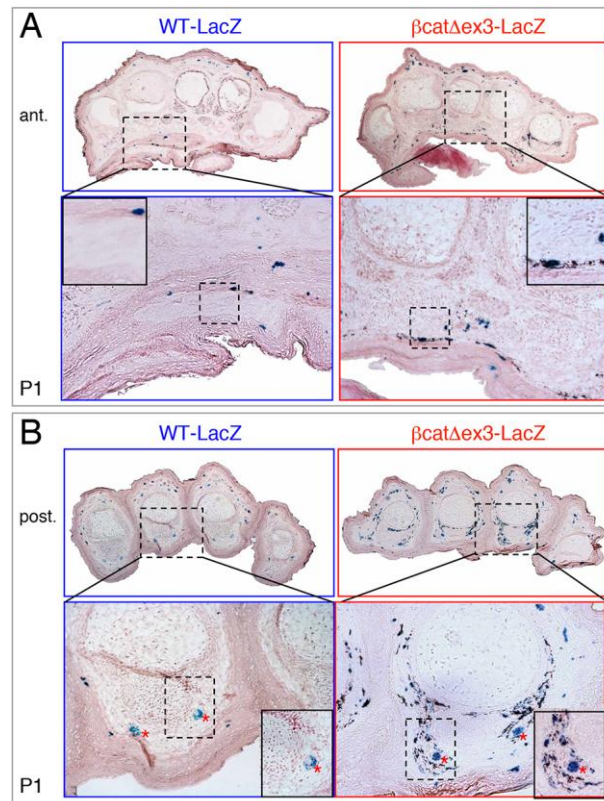


Figure 2. Overexpression of an active form of β -catenin induces hyperpigmented Dct-positive cells on the ventral side of the paws.

WT-LacZ and β cat Δ ex3-LacZ P1 paws were transversally sectioned, and X-gal and eosin stained. (A) Anterior (ant.) and (B) posterior (post.) paws at the metacarpal and phalangeal levels, respectively. In the dermis, mutant paws display high numbers of Dct-positive cells (melanocytes stained in blue, directly under the dermo-epidermal junction of the palmoplantar side of the paws (A) and around the bones of the digits (B). Note that these cells show high accumulation of melanin. In the dermis, WT paws contain a very low number of Dct-positive cells or pigmentation. Note that some nerves are stained in blue in the posterior paws (red asterisk) in WT and mutant paws. WT-LacZ = ($^{\circ}/^{\circ}$; β catex3 $^{flox/+}$; Dct::LacZ $^{\circ}$); β cat Δ ex3-LacZ = (Tyr::Cre $^{\circ}$; β catex3 $^{flox/+}$; Dct::LacZ $^{\circ}$).

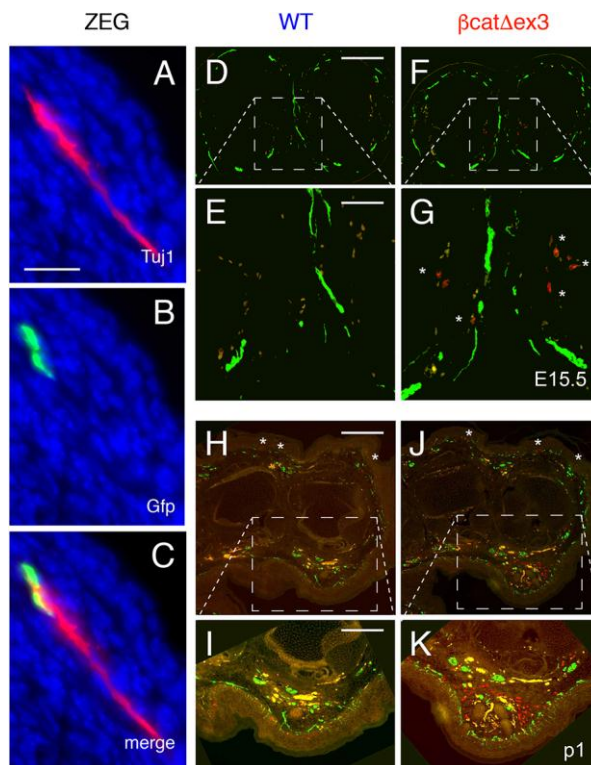


Figure 3. Gfp and Pmel positive cells are associated with TUJ1 positive cells during embryonic development

(A-C) Forelimb of $Tyr::Cre/^\circ$; $ZEG/^\circ$ (ZEG) E14.5 embryo was immunostained with (A) TuJ1 in red, (B) GFP in green antibodies, and counterstained with DAPI. Merge is presented in (C). WT (D,E,H,I) and $\beta cat\Delta ex3$ (F,G,J,K) E15.5 (D-G) and P1 (H-K) paws were transversally sectioned, and immunostained for Pmel (red) and TuJ1 (green). The yellow staining corresponds to red blood cells (unspecific labeling). Asterisks highlight the presence of melanocytes in G,H,J. Scale bar for A-C: 20 μm . Scale bars = 200 μm for D,F, Scale bars = 60 μm for E,G, Scale bars = 200 μm for H,J, Scale bars = 100 μm for I,K. Note that some TuJ1 positive cells are closed to Pmel positive cells. WT- = ($^\circ/^\circ$; $\beta catex3^{floX/+}$); $\beta cat\Delta ex3$ = ($Tyr::Cre/^\circ$; $\beta catex3^{floX/+}$).

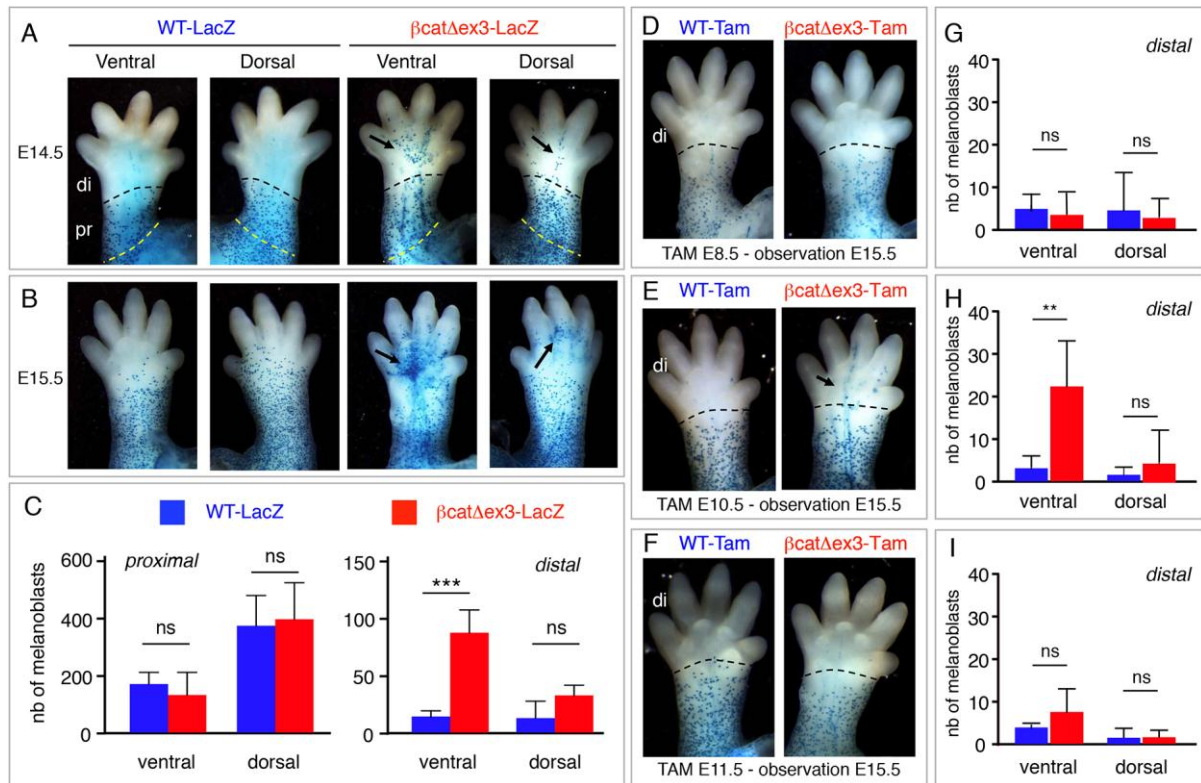


Figure 4. β -catenin favors the specification of SCPs towards melanoblasts.

(A-C) The number of melanoblasts is higher on the ventral side of the distal limbs of β cat Δ ex3 than WT mice. WT-LacZ and β cat Δ ex3-LacZ E14.5 (A) and E15.5 (B) paws were X-gal stained. Dorsal and ventral views are shown. The number of melanoblasts were estimated at E14.5 (C) in the distal (di) and proximal (pr) region of the limbs that are limited by dashed lines in (A). Arrows highlight ectopic melanoblasts. WT-LacZ = ($^{\circ}/^{\circ}$; β catex3 $^{fllox/+}$; Dct::LacZ $^{\circ}$); β cat Δ ex3-LacZ = (Tyr::Cre $^{\circ}$; β catex3 $^{fllox/+}$; Dct::LacZ $^{\circ}$). (D-I) Melanoblast numbers in the paws are increased when β -catenin is activated at E10.5. Ventral views of WT-Tam and β cat Δ ex3-Tam E15.5 paws induced with tamoxifen at E8.5 (D), E10.5 (E), and E11.5 (F) and X-gal stained. The number of melanoblasts was estimated at E15.5 in the distal (di) part of the paw that is delimited by the dashed lines in (D-F) after tamoxifen induction at E8.5 (G), E10.5 (H), and E11.5 (I). Arrow in (E) highlights ectopic melanoblasts. No X-gal positive cells were observed at E15.5 when Tam induction was performed at E12.5. WT-Tam = ($^{\circ}/^{\circ}$; β catex3 $^{fllox/+}$; Dct::LacZ $^{\circ}$); β cat Δ ex3-Tam = (Tyr::Cre-ER $^{T2}/^{\circ}$; β catex3 $^{fllox/+}$; Dct::LacZ $^{\circ}$). We followed a minimum of eight limbs for each situation. Using an impaired t-test *** = p-value < 0.001, ** = p-value < 0.01 ns = non significant.

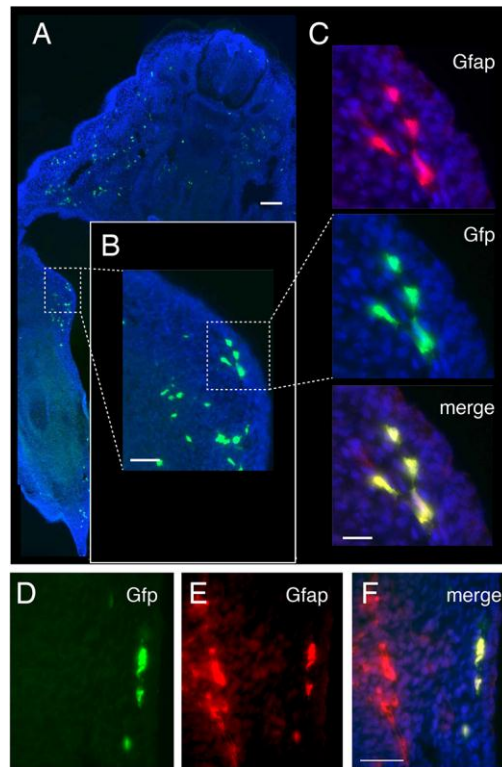


Figure 5. GFAP positive cells are defloxed in $Tyr::Cre^{+/+}; ZEG^{0/0}$ mice during embryonic development

(A) Transversal section at the level of the forelimb of a E14.5 $Tyr::Cre^{+/+}; ZEG^{0/0}$ embryo subjected to immunofluorescence to reveal GFP (green) and counter stained with DAPI (blue). GFP is produced in cells that were defloxed by the Cre recombinase. To create this panel, several images of the same embryo section were taken separately and assembled using Photoshop. Enlargement of one zone is shown in panel B (white rectangle). (C) Proximal parts of the ventral part of forelimb of $Tyr::Cre^{+/+}; ZEG^{0/0}$ embryo was immunostained with Gfap (red) and Gfp (green) antibodies, and counterstained with DAPI. (D-F) Distal parts of the ventral part of forelimb of $Tyr::Cre^{+/+}; ZEG^{0/0}$ embryo immunostained with Gfp in green (D) and Gfap in red (E) antibodies, and counterstained with DAPI. Merge is presented in F. Note that, in panels D-F, the majority of the defloxed cells (Gfp-positive) present in the distal part of the forelimb are producing Gfap, but Gfap positive cells can be either defloxed or not. Scale bars: 100 μ m for A, 25 μ m for B, 10 μ m for C, and 50 μ m for D-F.

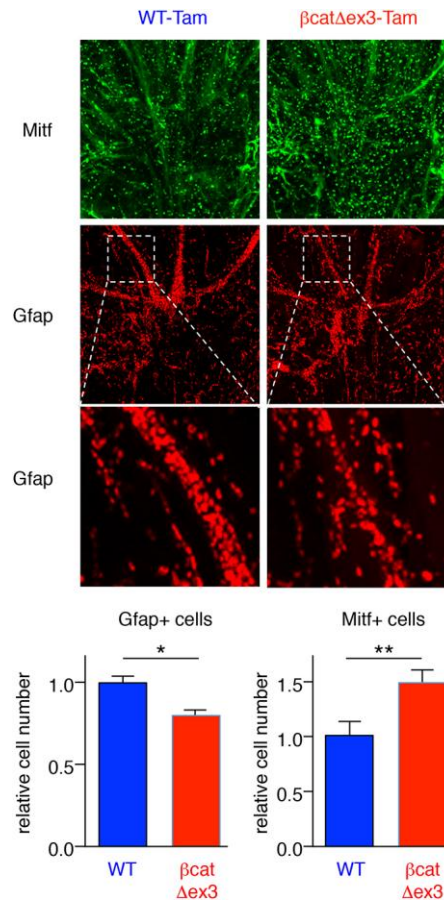


Figure 6. The number of paw melanoblasts increases at the expense of glial cells when β -catenin is activated at E10.5

Ventral views of WT-Tam and $\beta\text{cat}\Delta\text{ex3-Tam}$ E15.5 anterior paws from embryos induced with tamoxifen at E10.5. Immunostainings for Mitf-M (green) and Gfap (red). A zoom at the level of the nerve is presented and highlights the reduction of Gfap positive cells in $\beta\text{cat}\Delta\text{ex3}$ paws compared to WT. WT-Tam = ($^{\circ}/^{\circ}$; $\beta\text{catex3}^{\text{flox}/+}$); $\beta\text{cat}\Delta\text{ex3-Tam}$ = ($\text{Tyr}::\text{Cre-ER}^{\text{T2}/\circ}$; $\beta\text{catex3}^{\text{flox}/+}$). The relative amounts of Gfap positive (Gfap +) and Mitf positive (Mitf +) cells are shown (WT vs. $\beta\text{cat}\Delta\text{ex3}$). Note that it is a 3D reconstruction; there is an accumulation of the signal over and below the nucleus. We followed six limbs for each situation. Statistical analysis was performed using an unpaired t-test. Error bars correspond to SEM. * $p < 0.05$ and ** $p < 0.01$.

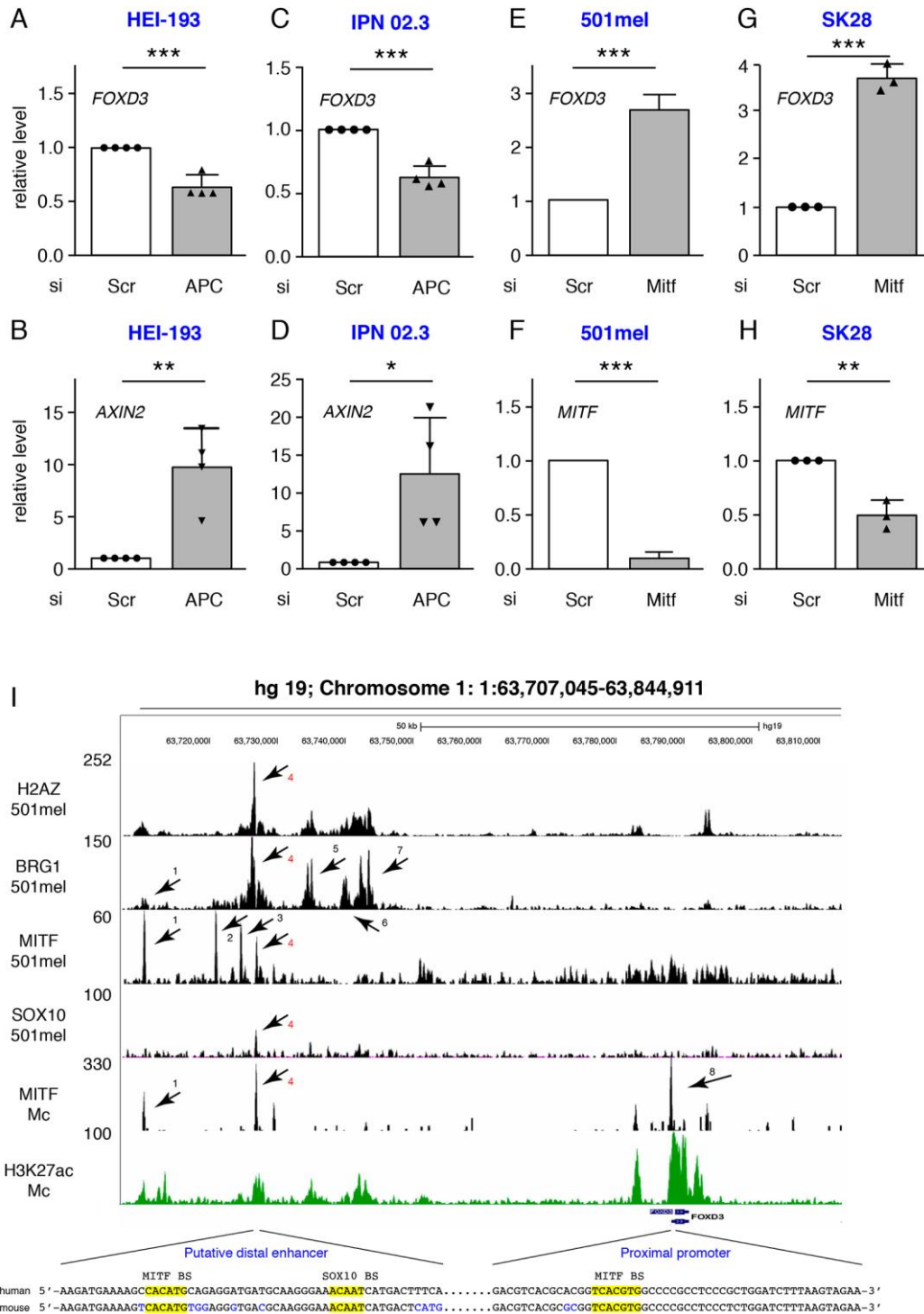


Figure 7. MITF represses *FOXD3* expression

(A-D) The relative amounts of *FOXD3* and *AXIN2* were determined by RT-qPCR from the HEI-193 schwannoma and IPN 02.3 Schwann cell lines after siRNA mediated knockdown of APC. (E-H) The relative amounts of *FOXD3* (E,G) and *MITF* (F,H) were determined by RT-qPCR in 501mel and SK28 human melanoma cell lines after siRNA mediated knockdown of *MITF*, respectively. (I) UCSC screenshot of ChIP-seq data at the *FOXD3* locus. Shown are ChIP-seq data for H2AZ, BRG1 MITF and SOX10 in 501mel melanoma cells as previously

described (GSE GSE61967) and for H3K27ac from GSM958157 (Laurette et al., 2015). MITF ChIP-seq in primary melanocytes (GSE50686) is from (Webster et al., 2014). Binding sites are indicated by arrows in the proximal promoter in primary melanocytes (Mc) and in a putative distal enhancer in Mc and 501mel cells. The DNA sequences under the peaks are shown along with the syntenic regions from mouse. MITF and SOX10 binding sites (BS) are highlighted in yellow. Each of these BS are bound by BRG1 and H2AZ; additional marks of regulatory sequences. Statistical analysis was performed using the unpaired t-test. Error bars correspond to SD. **p < 0.01 and ***p<0.001.

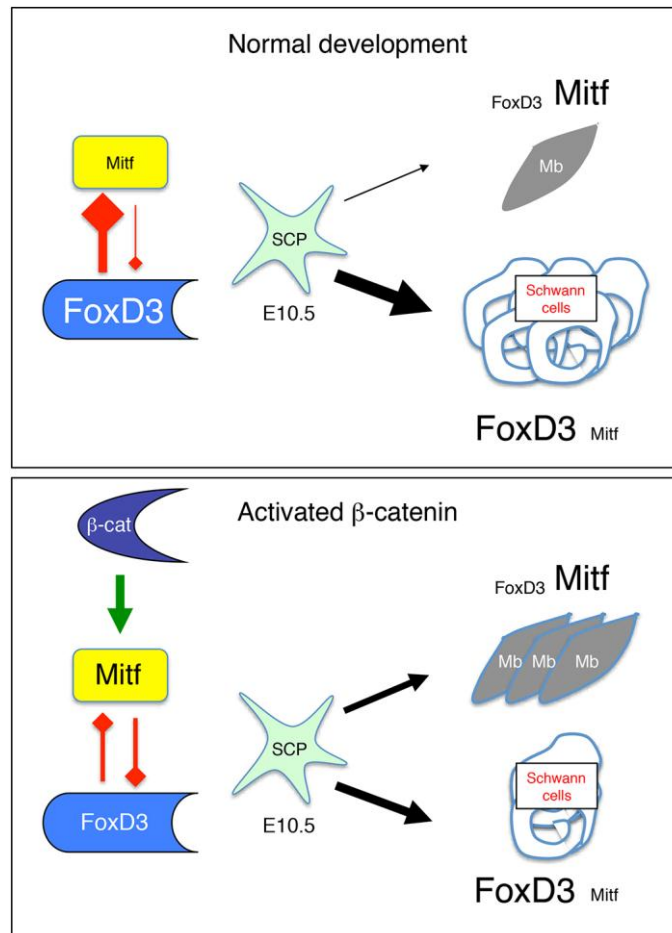


Figure 8. Schematic of the determination of SCP to generate Schwann cells and melanoblasts

FoxD3 and Mitf would regulate each other to specify Schwann cell and melanocyte lineage from SCP around E10.5. In the presence of a high content of FoxD3 and low content of Mitf, SCP would be directed towards the Schwann cell lineage and in the opposite; SCP would be directed towards the melanocyte lineage. In a situation in which β -catenin is activated, Mitf would be induced in SCP to promote more efficiently the specification of melanocyte, and repressing FoxD3 to specify less Schwann cells.

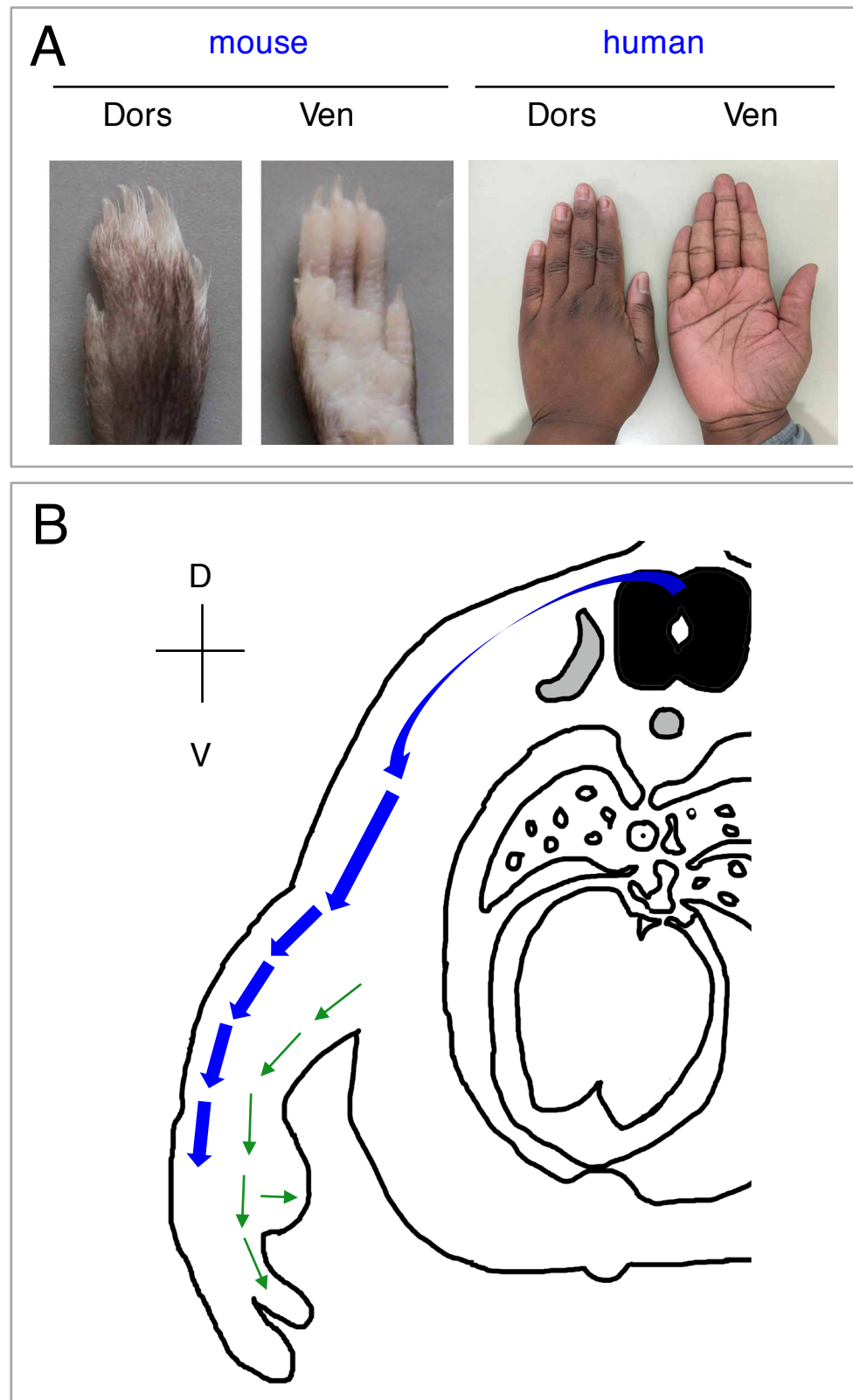


Fig. S1. Human and mouse pigmentation of the limb extremities

(A) Human and mouse palms are depigmented due to a low number of melanocytes. Back of the human and mouse extremities are pigmented. (B) Schematic of the migration of melanoblasts represented on a transversal section at the level of the limb. Blue arrows represent the migration path of the melanoblasts of the first wave (asymmetric and dorso-lateral). Green arrows represent the migration path of the melanoblasts of the second wave (asymmetric, dorso-ventral and derived from the Schwann cell precursors - SCP). D = dorsal. V = ventral.

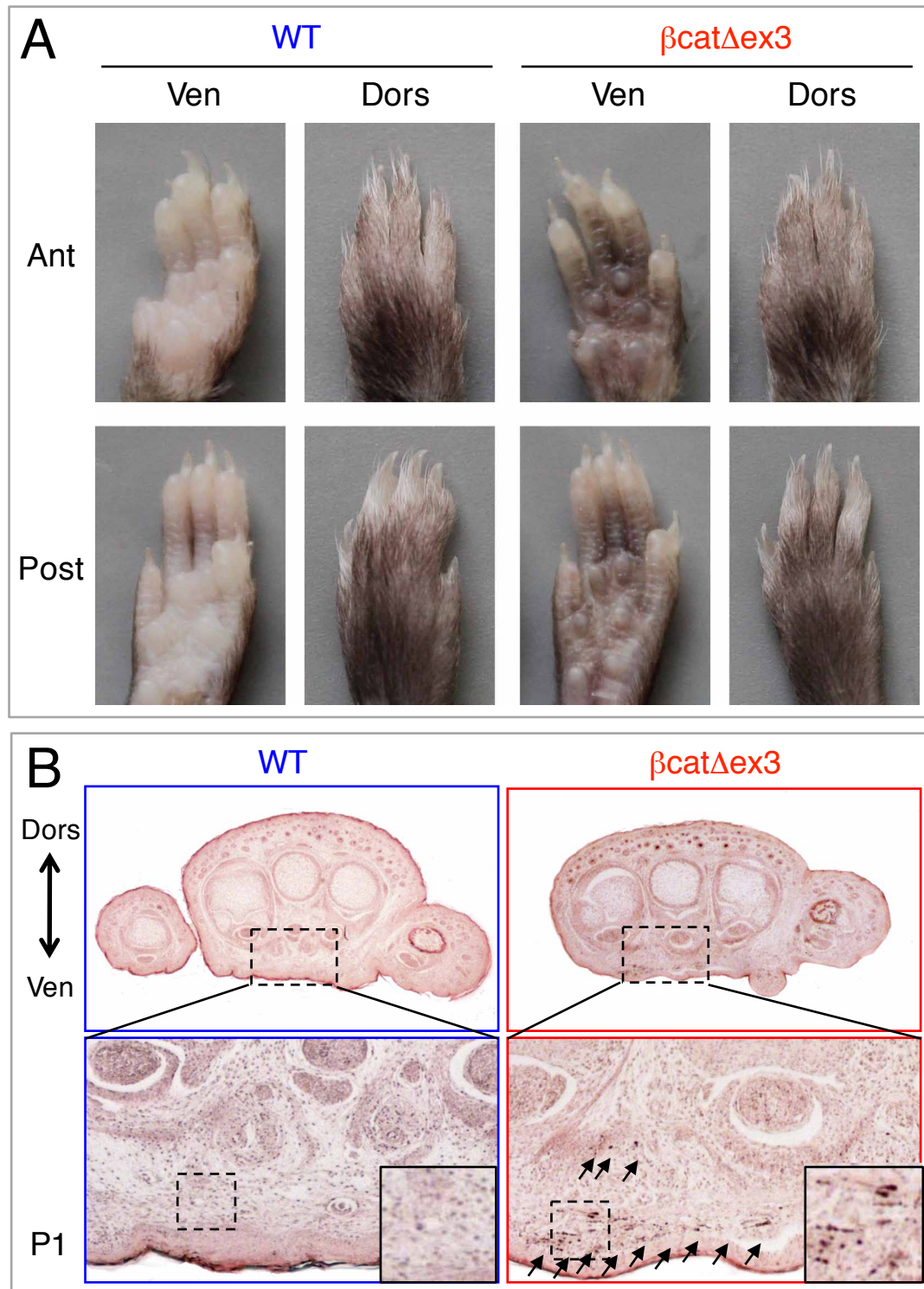


Fig. S2. The expression of an active form of β -catenin induces an accumulation of pigment on the palmoplantar side of the paws.

(A) Ventral (Ven) and dorsal (Dors) views of WT and $\beta\text{cat}\Delta\text{ex3}$ anterior (Ant) and posterior (Post) paws in adult mice. Note that the hyperpigmentation on the dorsal side of the paws is rarely visible. (B) Eosin staining of P1 (postnatal day 1) transversal paw sections at the metatarsal level. Arrows are pointing at melanin pigment. Note that no pigment is observed in the WT counterpart. WT = ($^{\circ}/^{\circ}$; $\beta\text{catex3flox}/+$) or (Tyr::Cre; $\beta\text{catex3}/+$). $\beta\text{cat}\Delta\text{ex3}$ = (Tyr::Cre/ $^{\circ}$; $\beta\text{cat}\Delta\text{ex3flox}/+$).

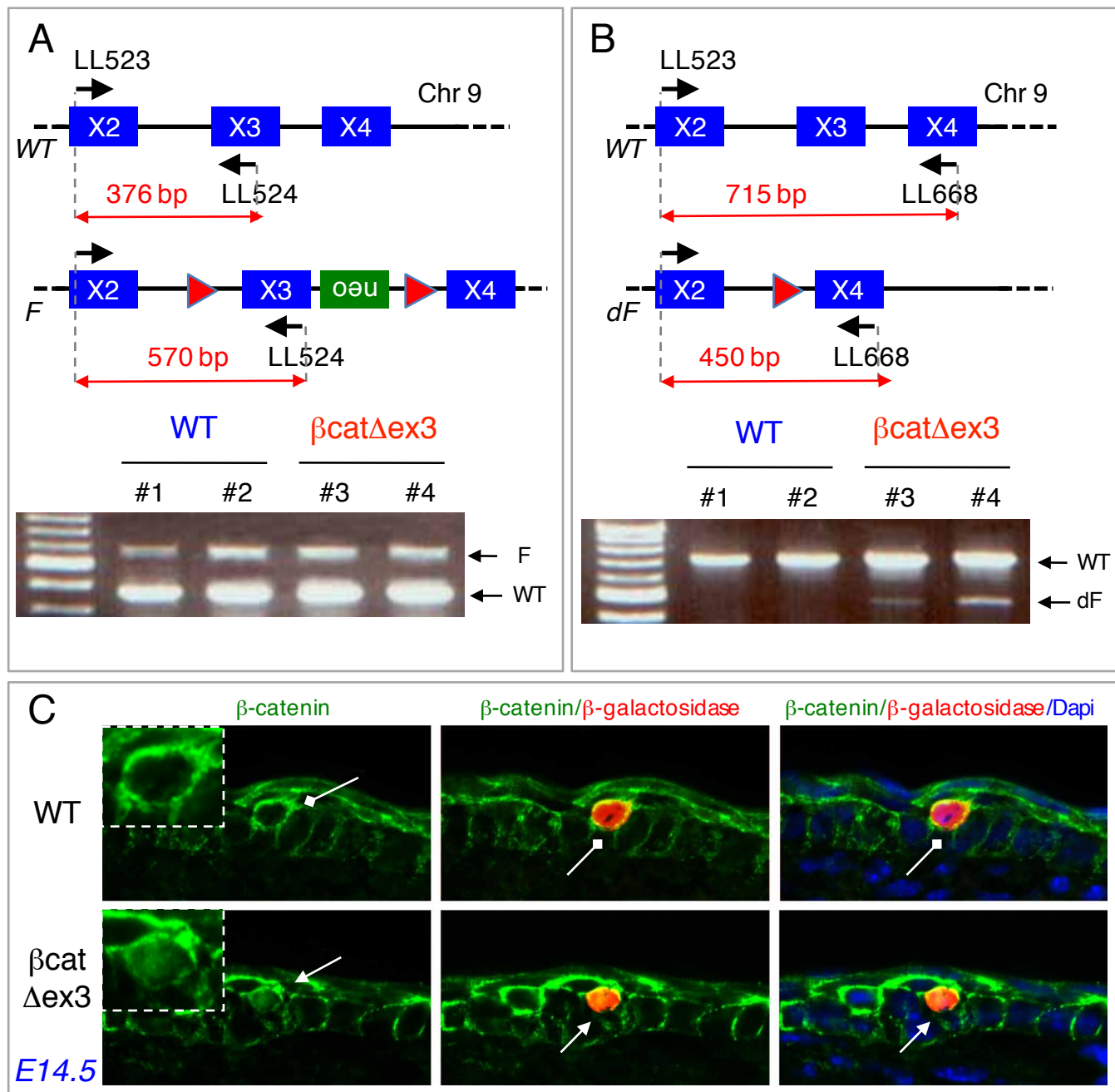


Fig. S3. β -catenin is defloxed after Cre recombination and localized in the nucleus of mutant melanoblasts and melanocytes.

(A,B) Schematic representation of the WT, floxed (F) and defloxed (dF) β -catenin locus. β -catenin is localized on chromosome (Chr) 9 in the mouse. A series of oligonucleotides (LL523, LL524, and LL668) was used to reveal the status of the β -catenin locus. (A) WT locus leads to a 376 bp band, and F locus to a 570bp band using the pair LL523 and LL524. (B) WT locus leads to a 715 bp band, and dF locus to a 450bp band using the pair LL523 and LL668. (C,D) Immunostaining with antibodies directed against β -catenin and β -galactosidase. Nuclei were stained with Dapi. β -galactosidase labels the Dct::LacZ-positive melanoblasts/melanocytes. (C) E14.5 WT and β cat Δ ex3 embryo sections. WT = ($^{\circ}/^{\circ}$; β catex3flox/+; Dct::LacZ $^{\circ}$); β cat Δ ex3 = (Tyr::Cre $^{\circ}$; β catex3flox/+; Dct::LacZ $^{\circ}$).

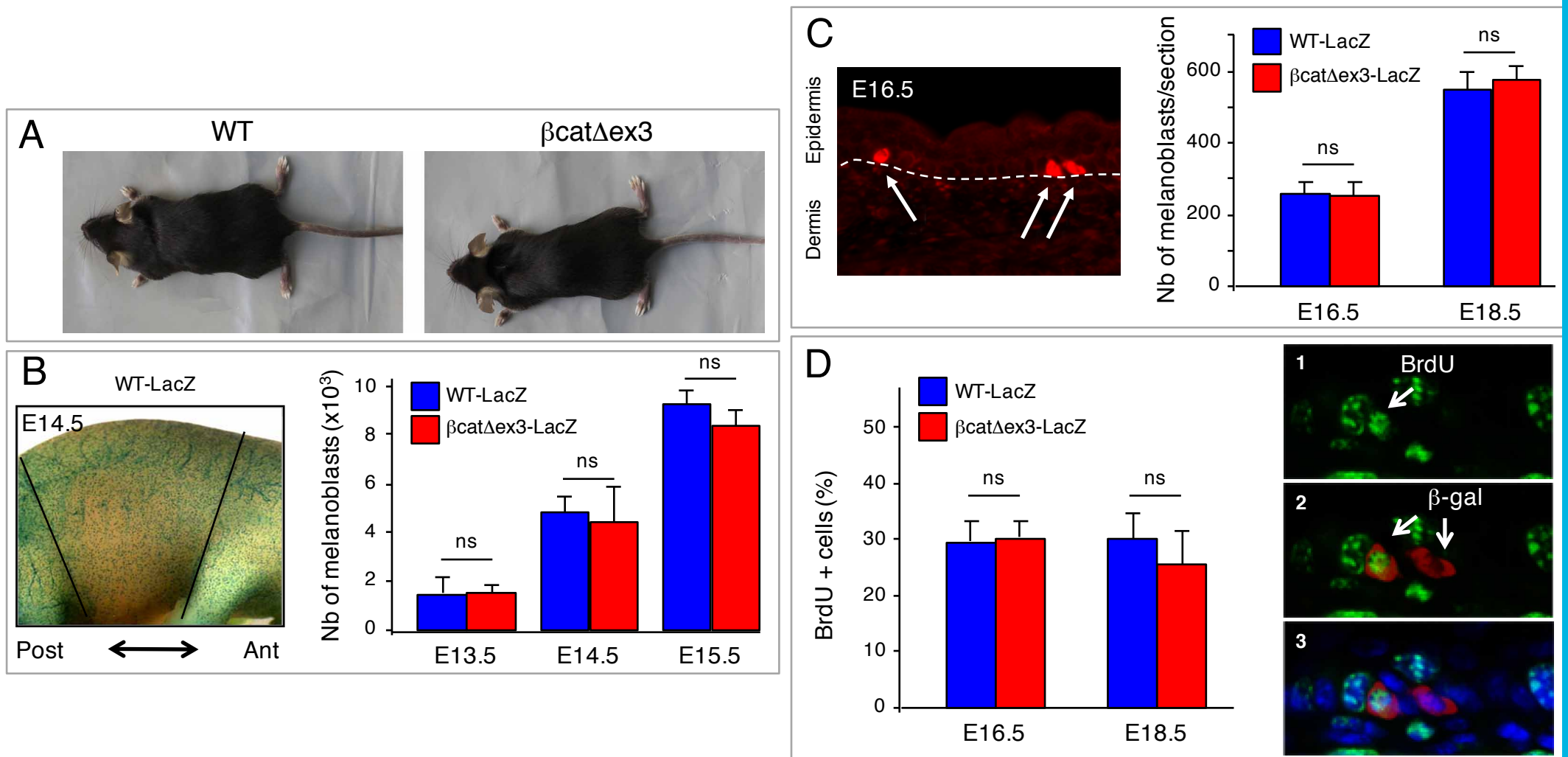


Fig. S4. The melanocyte lineage of the dorso-lateral wave is not perturbed in $Tyr::Cre^o$; β catex3flox/+ mice.

(A) Adult β cat Δ ex3 mice have the same coat/tail/ear color as control C57BL/6 mice. (B,C) β -catenin overexpression does not increase the number of truncal melanoblasts during embryonic development. (B) Macroscopic observations of WT-LacZ and β cat Δ ex3-LacZ embryos at E14.5 with the melanoblasts stained with X-gal for β -galactosidase activity. At E13.5, E14.5 and E15.5, the number of melanoblasts was estimated on the right side of the trunk region located between the forelimbs and hindlimbs (somites 13-25, limits shown as black lines the picture). (C) At E16.5 and E18.5, melanoblasts (red on photomicrographs and highlighted with white arrows) were counted on WT-LacZ and β cat Δ ex3-LacZ embryo sections immunostained for β -galactosidase. The numbers represent the melanoblasts located in the epidermis and hair follicles. (D) Determination of proliferation rate for β -galactosidase-positive cells at E16.5 and E18.5 in WT-LacZ and β cat Δ ex3-LacZ embryos. Between 15 and 54 sections, derived from two to four embryos from independent litters, were analyzed for each embryonic stage and each genotype. The percentages were obtained from melanoblasts of the epidermis and hair follicles. Immunofluorescence photomicrographs of a typical section show BrdU-positive cells in green (1), β -galactosidase-positive cells in red (2), and nuclei stained with Dapi in blue (3). Statistical significance was calculated with the Mann-Whitney U test and is indicated: ns, non significant. Post = posterior. Ant = anterior. WT = ($^o/^o$; β catex3flox/+) or ($Tyr::Cre$; β catex3+/+); β cat Δ ex3 = ($Tyr::Cre^o$; β catex3flox/+); WT-LacZ = ($^o/^o$; β cat Δ ex3flox/+; Dct::LacZ o); β cat Δ ex3-LacZ = ($Tyr::Cre^o$; β catex3flox/+; Dct::LacZ o).

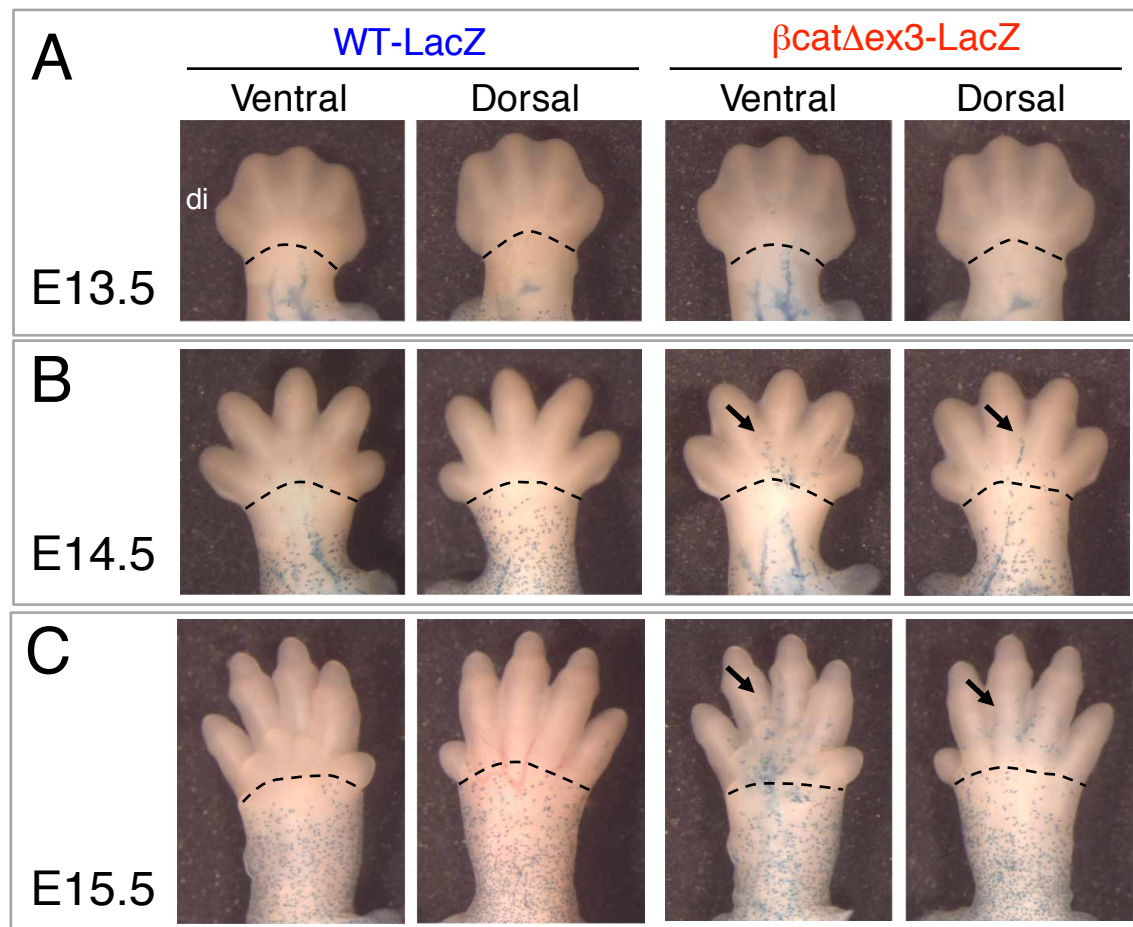


Fig. S5. Mutant melanoblasts are present in the distal region of the paws from E14.5. WT-LacZ and β cat Δ ex3-LacZ embryonic paws were stained with X-gal. At E13.5 (A), no melanoblast is observed in either WT or mutant distal (di) region of the paws. At E14.5 (B) and E15.5 (C) β cat Δ ex3-LacZ melanoblasts are found in the distal part of the of the anterior paws. No melanoblast is observed in WT (B,C). Dashed lines separate the distal (di) part of the limb (paw) from the proximal limb. Arrows indicate the presence of melanoblasts. WT-LacZ = ($^{\circ}/^{\circ}$; β catex3flox/+; Dct::LacZ/ $^{\circ}$); β cat Δ ex3-LacZ = (Tyr::Cre/ $^{\circ}$; β catex3flox/+; Dct::LacZ/ $^{\circ}$).

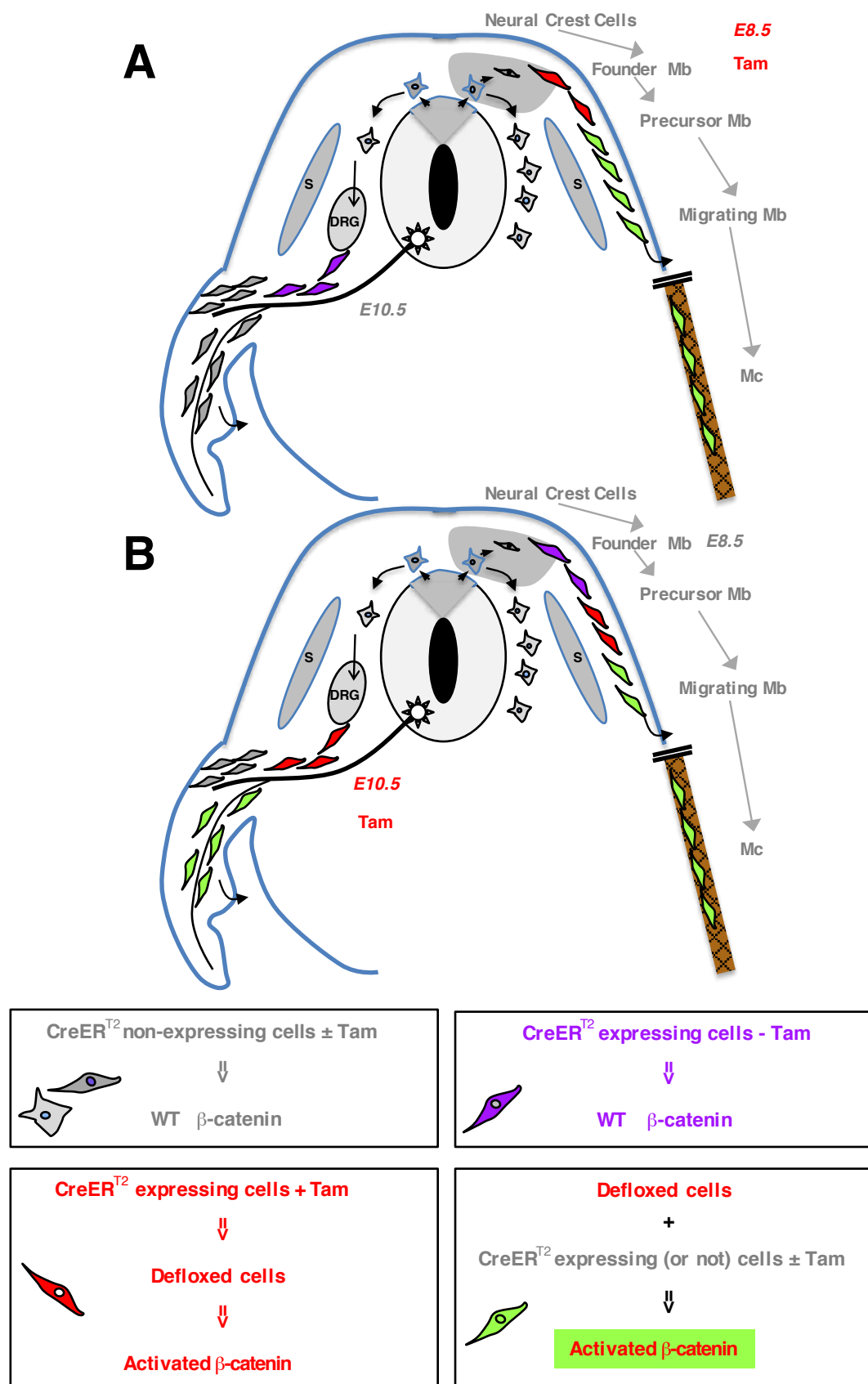


Fig. S6. Activation of β -catenin in the first and/or second waves of melanocytes

The Cre-ERT2 recombinase mRNA and protein are present in cells in which the tyrosinase promoter is active. Cre-ERT2 protein is active in the presence of 4OH-tamoxifen, allowing this chimeric protein to be translocated to the nucleus and to deflox in an irreversible way the floxed gene. In consequence, once the gene is defloxed, all the descendent cells will remain defloxed. The temporal activation of Cre-ERT2 is crucial for the fate of the floxed status of the melanocyte lineage. Cre-ERT2 expressing cells may induce the activation of β -catenin in the presence of tamoxifen (red). However, cells expressing Cre-ERT2 will not be defloxed in the absence of tamoxifen (purple). Cells that have been defloxed, and their descendants, are expressing an activated form of β -catenin (green). Cells that do not express Tyrosinase, and their ascendants, will never produce an activated form of β -catenin (grey). Tamoxifen was injected in pregnant mother when the embryos were E8.5 (A) or E10.5 days old (B). Tamoxifen induction occurring at E8.5 allows the activation of β -catenin in the first wave, but not in the second wave of melanocytes. At E10.5, Tamoxifen induction occurs at the time of the specification of SCP. In wild-type conditions, they are normally specified in Schwann cell but occasionally may generate some melanocytes.